
Self-CriTeach: LLM Self-Teaching and Self-Critiquing for Improving Robotic Planning via Automated Domain Generation

Jinbang Huang¹, Zhiyuan Li^{1,2}, Yuanzhao Hu^{1,3}, Zhanguang Zhang¹, Mark Coates⁴,
 Xingyue Quan¹, Yingxue Zhang¹

¹Huawei Noah’s Ark Lab, ²University of Toronto,

³University of British Columbia, ⁴McGill University,

Abstract

Large Language Models (LLMs) have recently shown strong promise for robotic task planning, particularly through automatic planning domain generation. Planning domains are brittle under imperfect logical states and perception noise; prior approaches largely treat generated planning domains as plan utilities, overlooking their potential as scalable sources of reasoning supervision and structured reward signals. At the same time, reasoning LLMs depend on chain-of-thought (CoT) supervision that is expensive to collect for robotic tasks, and reinforcement learning (RL) faces challenges on reward engineering. We propose Self-CriTeach, an LLM self-teaching and self-critiquing framework in which an LLM autonomously generates symbolic planning domains that serve a dual role: (i) enabling large-scale generation of robotic planning problem–plan pairs, and (ii) providing structured reward functions. First, the self-written domains enable large-scale generation of symbolic task plans, which are automatically transformed into extended CoT trajectories for supervised fine-tuning. Second, the self-written domains are reused as structured reward functions, providing dense feedback for reinforcement learning without manual reward engineering. This unified training pipeline yields a planning-enhanced LLM with higher planning success rates, stronger cross-task generalization, reduced inference cost, and resistance to imperfect logical states.

1 Introduction

Large Language Models (LLMs) have shown strong potential in robotic task planning due to their reasoning capabilities and cross-task generalization (Huang et al., 2022b,a; Wang et al., 2024; Li et al., 2023; Zhao et al., 2024). However, LLM-based planners often suffer from stochastic outputs and error accumulation over long-horizon tasks, leading to failures. To address these issues, prior work has combined LLMs with symbolic search-based algorithms to improve long-horizon planning robustness (Meng et al., 2024; Hu et al., 2023; Liu et al., 2023). More recently, LLMs have been used to automatically infer planning domains (Oswald et al., 2024; Byrnes et al., 2024; Guan et al., 2023; Han et al., 2024b; Huang et al., 2025b). While effective, these approaches primarily treat inferred planning domains as search utilities, overlooking their potential as scalable sources of reasoning supervision and structured feedback for reinforcement learning (RL) (Dalal et al., 2023; Khodeir et al., 2023). As a result, symbolic planning remains largely external to the learned model, resulting in brittleness when faced with imperfect logical states and perceptual noise. This limitation motivates learning-based planners that internalize symbolic planning structure and exhibit resistance to imperfect or noisy logical state representations.

A natural path toward such internalization is suggested by recent advances in reasoning-oriented LLMs, which have advanced substantially through a combination of chain-of-thought (CoT) super-

vised fine-tuning (SFT) and reinforcement learning (RL)-based post-training (Wei et al., 2022; Cobbe et al., 2021; Zelikman et al., 2022; Schulman et al., 2017; Shao et al., 2024; Wang et al., 2025b). This SFT + RL paradigm has emerged as a verified and effective pathway for bootstrapping LLM reasoning capability. However, applying this paradigm to robotic planning remains challenging. First, CoT supervision in robotics typically requires large-scale, manually curated reasoning traces, which are costly and difficult to obtain. Second, RL-based improvement is hindered by the lack of structured and scalable reward functions, as robotic tasks involve long-horizon, combinatorial decision-making with sparse rewards (Gupta et al., 2019; Kulkarni et al., 2016).

Planning domains offer a promising bridge between these challenges. Prior work has shown that symbolic planning can generate scalable robot task plans (Dalal et al., 2023), and transformation between symbols and languages is effective (Pan et al., 2023a; Han et al., 2024a; Tafjord et al., 2021; Wang et al., 2025a). In parallel, the structured nature of symbolic planning domains makes them well suited to serve as systematic dense reward signals for improving model performance. Building on these insights, we posit that LLM self-written planning domains provide a unified solution for both supervision and feedback in robotic planning.

We propose SELF-CRITEACH, a self-teaching and self-critiquing framework that reinterprets LLM self-generated planning domains as data sources and training signals rather than mere planning tools. Specifically, symbolic planning domains in Planning Domain Definition Language (PDDL) format, automatically generated by the LLM, fulfill two roles: (1) generate executable task plans that are transformed into context-rich CoT trajectories for supervised fine-tuning; and (2) serve as structured, dense reward functions that enable self-critiquing and reinforcement learning without manual reward engineering. Our contributions include:

SELF-CRITEACH Framework: We introduce SELF-CRITEACH, a novel automated framework that treats LLM self-generated PDDL planning domains as reusable knowledge sources, whose compositional structure enables both scalable generation of planning supervision for self-teaching and structured reward signals for self-critiquing via RL.

Self-teaching via data generation: SELF-CRITEACH allows the base LLM to produce validated long-horizon planning datasets that extend beyond its intrinsic planning capacity, and to use this data for SFT without human annotation.

Automatic symbolic–CoT transformation: We introduce an automatic CoT generation procedure that translates robot symbolic plans and states into a CoT reasoning trace using the base LLM, and empirically demonstrate the effectiveness of the CoT in self-teaching.

Self-critiquing with planning domains: The system reuses the self-generated PDDL planning domains as structured reward functions, enabling post RL training without manual reward engineering.

Empirical gains: SELF-CRITEACH produces a planning-enhanced LLM that achieves robust planning performance, stronger cross-task generalization, reduced inference token costs, and resistance to imperfect logical estimation.

2 Related Work

Learning to plan LLMs have emerged as powerful tools for robotic task planning (Huang et al., 2022b,a; Wang et al., 2024; Chen et al., 2024; Li et al., 2023; Zhao et al., 2024). Early work treated LLMs as direct planners, but such approaches struggle with long-horizon dependencies and error accumulation (Sermanet et al., 2023; Driess et al., 2023; Brohan et al., 2022; Chen et al., 2023; Wang et al., 2024). Subsequent methods use LLMs to guide symbolic search, improving exploration efficiency while preserving planning completeness (Zhao et al., 2024; Yang et al., 2025a; Meng et al., 2024; Hu et al., 2023; Silver et al., 2024), yet they rely on manually engineered planning domains or search structures, limiting scalability. A complementary line of work studies automatic planning domain generation in PDDL (McDermott et al., 1998), where symbolic world models are learned from data or inferred by LLMs through interaction. Existing approaches either refine partial domains (Diehl et al., 2021; Kumar et al., 2023; Silver et al., 2023; Liang et al., 2024; Athalye et al., 2024; Byrnes et al., 2024; Wong et al., 2023; Liu et al., 2024; Zhu et al., 2024; Huang et al., 2025a), construct domains from natural-language descriptions (Guan et al., 2023; Han et al., 2024b; Oswald et al., 2024), or induce domains directly from demonstration trajectories (Huang et al., 2025b). While these results establish LLMs as capable domain generators, prior work largely treats PDDL

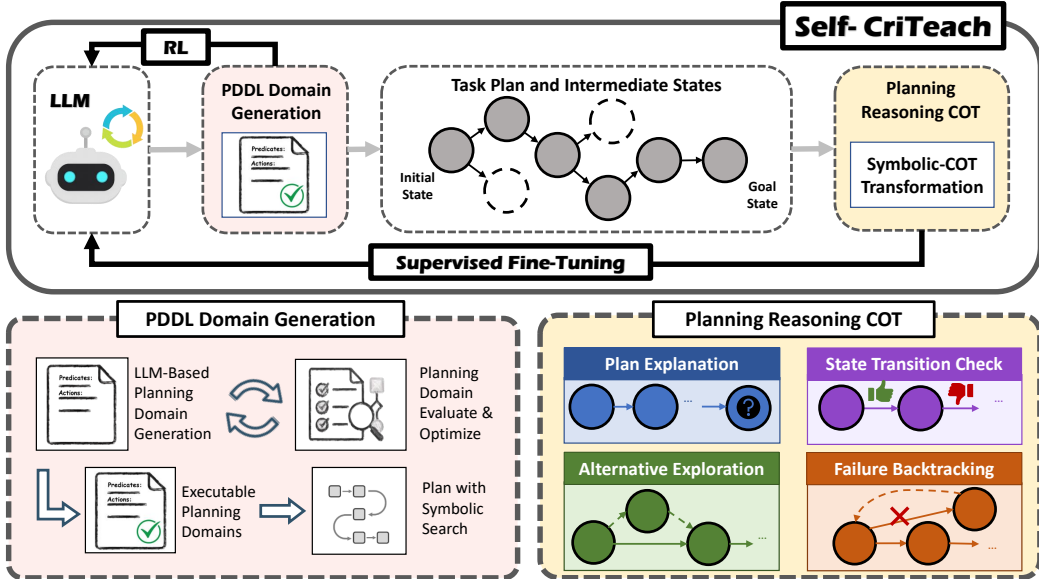


Figure 1: Overview of the proposed SELF-CRITeach framework. The base LLM first generates and iteratively refines PDDL planning domains, which are used to perform symbolic search and produce task plans with intermediate states. These plans are converted into chain-of-thought traces by the same base LLM by including plan explanation, state-transition checking, alternative exploration, and failure backtracking. The resulting CoT data is first used for supervised fine-tuning, after which the same self-written planning domains provide structured reward signals for reinforcement learning. Together, supervised and reinforcement learning enable the model to internalize symbolic planning behavior, yielding a reasoning-enhanced LLM with improved generalization and long-horizon reasoning.

domains as planning utilities, overlooking their potential as scalable sources of verified reasoning data. Motivated by recent evidence that PDDL can supervise robot motion learning (Dalal et al., 2023; Khodeir et al., 2023), we propose a self-improving framework that leverages LLM-generated planning domains as training data, yielding substantial performance gains.

Reasoning LLM and Post-training Early progress in LLM reasoning primarily relied on few-shot prompting, which are proven effective for simple tasks but struggle with complex multi-step reasoning (Brown et al., 2020). Chain-of-thought (CoT) prompting elicits intermediate reasoning steps, yielding substantial performance gains (Wei et al., 2022; Kojima et al., 2022). Moreover, a range of inference-time strategies—such as self-consistency and tree-based search—have further improved reasoning robustness (Wang et al., 2023b; Yao et al., 2023). Beyond prompting, supervised fine-tuning (SFT) has been widely adopted in model training (Ouyang et al., 2022; Cobbe et al., 2021). In particular, correctness-validated and self-refined rationales have led to significant improvements (Zelikman et al., 2022; Yuan et al., 2023; Tong et al., 2024; Lee et al., 2025; Hosseini et al., 2024; Wang et al., 2025b). More recently, reinforcement learning (RL) has emerged as a key component of reasoning-oriented post-training (Schulman et al., 2017; Shao et al., 2024; Achiam et al., 2017), with combined SFT+RL pipelines demonstrating superior performance (Christiano et al., 2017; Ouyang et al., 2022; Rafailov et al., 2023; Wang et al., 2025b). Symbolic logic has been explored as a means of enhancing the reasoning capacities of LLMs. Prior work has investigated symbol–language transformations to enable logical reasoning in language models (Pan et al., 2023a; Han et al., 2024a; Olausson et al., 2023; Xu et al., 2024; Pan et al., 2023b; Liu et al., 2023; Tafjord et al., 2021). However, symbolic reasoning traces are often difficult for LLMs to interpret directly (Wang et al., 2025a; Feng et al., 2024), particularly in robotics, where physical constraints are expressed in symbolic form. Recent studies further reveal a misalignment between symbolic traces and natural-language reasoning (Stechly et al., 2024), limiting their effectiveness as direct supervision for LLM training. To bridge this gap, we propose an automatic symbolic-to-CoT transformation

method based on LLM self-alignment. We show that this transformation is critical for transferable learning and improves the planning performance of fine-tuned LLMs.

3 Preliminaries

A PDDL domain is defined by $\mathcal{D} = (\mathcal{P}, \mathcal{A})$, where \mathcal{P} is a set of predicates and \mathcal{A} is a set of actions. The object set is defined as $\mathcal{O} = \{o_1, \dots, o_n\}$. Each **predicate** $p \in \mathcal{P}$ describes object properties or relations characterized by a Boolean classifier $p(o_1, \dots, o_i) \rightarrow \{0, 1\}$. Instantiating p with objects $o_1, \dots, o_i \in \mathcal{O}$ yields a ground atom. Let $\mathcal{G} = \{p(o_1, \dots, o_k) \mid p \in \mathcal{P}, o_i \in \mathcal{O}\}$ be the set of all possible ground atoms. A symbolic state is a set of true atoms, $\mathcal{X} \subseteq \mathcal{G}$. An **action** $a \in \mathcal{A}$ is defined as $a = \langle \text{PRE}, \text{EFF}^+, \text{EFF}^- \rangle$, where PRE denotes the predicates that must hold for the action to be applicable. The effects consist of add effects EFF^+ and delete effects EFF^- , which specify how the state is updated when the action is executed. Initiating a with concrete objects $o_1, \dots, o_j \in \mathcal{O}$ results in a ground action $a(o_1, \dots, o_j)$. Executing a induces the state transition $\mathcal{X}^t \times a \rightarrow \mathcal{X}^{t+1}$. Thus, a formal definition of a **planning problem** becomes,

$$\mathcal{Q} = \langle \mathcal{O}, \mathcal{D}, \mathcal{X}^{(init)}, \mathcal{X}^{(goal)} \rangle, \mathcal{D} = (\mathcal{P}, \mathcal{A}), \quad (1)$$

and a solution plan is a sequence of ground actions

$$\tau = \{a^{(0)}, \dots, a^{(T-1)}\} = \text{PDDLSolver}(\mathcal{Q}), \forall a^{(i)} \in \mathcal{A} \quad (2)$$

such that $\mathcal{X}^{(init)} \times \tau \rightarrow \mathcal{X}^{(goal)}$.

3.1 Automatic LLM Planning Domain Generation

Prior work has demonstrated that a base LLM \mathcal{M}_0 is capable of automatically generating planning domains from unstructured inputs such as natural language descriptions, task specifications, or demonstrations (Han et al., 2024b; Silver et al., 2023; Kumar et al., 2023; Huang et al., 2025b; Oswald et al., 2024; Guan et al., 2023). Formally, we have

$$\hat{\mathcal{D}} \triangleq (\hat{\mathcal{P}}, \hat{\mathcal{A}}), \quad (\hat{\mathcal{P}}, \hat{\mathcal{A}}) = \Psi^{\mathcal{M}_0}(\mathcal{U}), \quad (3)$$

where \mathcal{U} denotes the input source and $\hat{\mathcal{D}}$ is the generated domain with predicates $\hat{\mathcal{P}}$ and actions $\hat{\mathcal{A}}$. Ψ indicates the selected domain generation method. The resulting domain enables planning problems to be solved by symbolic search. Task plans are validated in simulation under physical constraints, assuming a predefined robot skill library.

3.2 From PDDL to CoT Generation

Given a generated domain $\hat{\mathcal{D}}$, the symbolic search naturally induces structured reasoning traces. A solution plan $\tau = \{a^{(0)}, \dots, a^{(T-1)}\}$ encodes a verifiable sequence of state transitions that can be expanded into stepwise natural-language explanations.

Symbolic trace. For a planning problem $\mathcal{Q} = \langle \mathcal{O}, \hat{\mathcal{D}}, \mathcal{X}^{(init)}, \mathcal{X}^{(goal)} \rangle$ and its solution τ , each ground action $a^{(t)}$ yields the ordered symbolic state transition trace

$$\mathcal{T}^{sym} = \{(\mathcal{X}^t, a^{(t)}, \mathcal{X}^{t+1})\}_{t=0}^{T-1}. \quad (4)$$

Natural-language trace. Each symbolic state transition trace $(\mathcal{X}^t, a^{(t)}, \mathcal{X}^{t+1})$ is then mapped by the base model \mathcal{M}_0 into a natural-language explanation:

$$e^{(t)} = f_{\text{NL}}^{\mathcal{M}_0}(\mathcal{X}^t, a^{(t)}, \mathcal{X}^{t+1}). \quad (5)$$

CoT trajectory. Concatenating these explanations yields the full CoT trajectory

$$\text{CoT}_\tau = \{e^{(0)}, e^{(1)}, \dots, e^{(T-1)}\}, \quad (6)$$

which explicitly aligns symbolic planning semantics with natural-language reasoning.

4 Problem Setting

We address the problem of improving a base language model \mathcal{M}_0 into a planning-enhanced model \mathcal{M}_{SCT} through the SELF-CRITTEACH framework. Given domain inference input \mathcal{U} , the base model \mathcal{M}_0 induces a symbolic planning domain $\hat{\mathcal{D}}$, on which a symbolic solver generates problem–plan pairs $\langle \mathcal{Q}, \tau \rangle$. Each plan τ is transformed into CoT explanations CoT_τ by \mathcal{M}_0 . The paired data are then concatenated into full reasoning traces $\zeta_{align} = \langle \mathcal{Q}, \tau, \text{CoT}_\tau \rangle$ which serve as training sources. Aggregated over tasks, the collection $\mathcal{C} = \{\zeta_{align}^i\}_{i=1}^N$ forms a corpus for model fine-tuning. Combining \mathcal{C} for SFT and $\hat{\mathcal{D}}$ as an RL reward signal, the system yields a model \mathcal{M}_{SCT} with improved planning ability, stronger generalization, reduced inference cost, and resistance to imperfect logical states.

5 Methodology

As shown in Figure 1, SELF-CRITTEACH is a self-teaching and self-critiquing framework that uses a base LLM \mathcal{M}_0 to generate and iteratively refine PDDL planning domains, which serve as scalable sources of verified supervision and structured reward signals. This section explains the methodology of SELF-CRITTEACH in four stages.

5.1 Automatic planning domain generation

The first stage of SELF-CRITTEACH focuses on automatically inducing robotic planning domains grounded in physical constraints, building on prior milestone approaches in domain induction. Given a robot task demonstration \mathcal{U} , the base LLM \mathcal{M}_0 infers predicates and action schemas by summarizing simulated robot–object interactions and compiles them into a PDDL planning domain $\mathcal{D} = \langle \hat{\mathcal{P}}, \hat{\mathcal{A}} \rangle$, following the domain generation framework of Huang et al. (2025b). While effective, this framework treats the induced domain as a one-shot output and lacks a feedback mechanism for continual refinement. To address this limitation, we introduce an explicit closed-loop domain correction procedure that incorporates feedback-driven refinement methods from Oswald et al. (2024); Han et al. (2024b). The generated domain is validated on sampled planning problems, and planner failure traces are lifted into structured diagnostic signals for \mathcal{M}_0 to perform targeted logical repairs. However, such feedback mechanisms primarily aim to restore feasibility rather than optimize domain compactness. Therefore, we additionally employ a hill-climbing algorithm over the domain structure to prune redundant components while preserving solvability (Silver et al., 2023; Kumar et al., 2023). This combined validation–repair–pruning loop yields compact, executable planning domains suitable for downstream learning. Additional details are provided in Section A.1.

5.2 Symbolic-CoT Transformation for Training

The next step transforms symbolic plans into chain-of-thought (CoT) representations by eliciting planner decision reasoning in natural language. This step is essential, as directly training LLMs on raw symbolic structures empirically leads to solution memorization and unstable generalization. Given a planning problem \mathcal{Q} and its solution plan τ , the base model \mathcal{M}_0 is prompted with a designed template that converts symbolic state–action transitions into grounded reasoning traces in four aspects. **Plan explanation** prompts the model to explicitly justify why each action is selected in terms of goal progression to expose the intermediate decision structure of symbolic search. **State transition checking** requires the model to verify that constraints, action preconditions, and resulting effects are correctly satisfied, enforcing global plan consistency through step-wise validity checks. **Alternative exploration** asks the model to enumerate other applicable actions at each state and reason about their potential effects and why they are not prioritized. **Failure backtracking** elicits reasoning over infeasible branches by tracing constraint violations back to earlier decisions. This structured elicitation converts symbolic plans into decision-centric CoT traces, enabling the model to internalize symbolic planning dynamics within its latent reasoning space and improving planning performance through fine-tuning.

To improve robustness and avoid overfitting to a single solution pattern, the planning domain is allowed to generate diverse valid solutions for the same problem. This augmentation exposes the model to varied planning strategies, reflecting trade-offs among plan optimality, reasoning depth, and

error recovery behaviors. The resulting dataset therefore captures a broad spectrum of structured reasoning patterns, providing rich supervision signals for SFT. Details of the prompt template are provided in Section A.3.2.

5.3 Supervised Fine-tuning

Each planning tuple comprises a planning problem, its symbolic plan, and the aligned CoT trace $\zeta = \langle \mathcal{Q}, \tau, \text{CoT}_\tau \rangle$, and the full training dataset is $\mathcal{C} = \{\zeta^i\}_{i=1}^N$. During SFT, the model is trained to generate both the action sequence τ and the explanatory trajectory CoT_τ conditioned on the input problem \mathcal{Q} . The training objective is the standard autoregressive language modeling loss:

$$\mathcal{L}_{\text{SFT}} = - \sum_{i=1}^N \sum_{t=1}^{T_i} \log P(y_{i,t} \mid \mathcal{Q}_i; \theta), \quad (7)$$

where T_i is the length of the supervised output sequence for the i -th instance, $y_{i,t}$ denotes the t -th token of the concatenated plan and reasoning trace $\langle \tau_i, \text{CoT}_{\tau_i} \rangle$, and θ denotes the model parameters. As shown in prior studies (Wang et al., 2025b; Ouyang et al., 2022), this process compels the model to produce accurate plans while producing coherent reasoning chains imitating the planning behavior.

5.4 Reinforcement Learning

The supervised fine-tuned model \mathcal{M}_{SFT} is further optimized through reinforcement learning using the self-generated planning domain as a structured reward signal. Unlike sparse success-based rewards, the planning domain provides fine-grained failure feedback, including precondition violations and goal mismatches, enabling step-level plan evaluation instead of binary success/failure signals.

We primarily adopt Constrained Policy Optimization (CPO) (Achiam et al., 2017), which formulates the policy update as a constrained optimization problem:

$$\begin{aligned} \pi_{k+1} &= \arg \max_{\pi} \mathbb{E}_{\tau \sim \pi} \left[\sum_{t=0}^T R(\mathcal{X}_t, a_t) \right] \\ \text{s.t. } \mathbb{E}_{\tau \sim \pi} \left[\sum_{t=0}^T C(\mathcal{X}_t, a_t) \right] &\leq d, \quad D_{\text{KL}}(\pi \parallel \pi_k) \leq \delta \end{aligned} \quad (8)$$

where π_k denotes the policy at iteration k , d is the constraint threshold, $D_{\text{KL}}(\cdot \parallel \cdot)$ is the KL-divergence between policies, and $\delta > 0$ controls the maximum step size of each policy update. The step-level reward $R(\mathcal{X}_t, a_t)$ quantifies goal predicate satisfaction at state \mathcal{X}_t :

$$R(\mathcal{X}_t, a_t) = \frac{|\mathcal{X}^{(\text{goal})} \cap \mathcal{X}_t|}{|\mathcal{X}^{(\text{goal})}|} \quad (9)$$

where constraint cost $C(\mathcal{X}_t, a_t)$ penalizes actions that violate domain preconditions or produce inconsistent states:

$$C(\mathcal{X}_t, a_t) = \mathbf{1}[\text{prec}(a_t) \not\subseteq \mathcal{X}_t] + \lambda \cdot \mathbf{1}[\neg \text{valid}(\mathcal{X}_{t+1})] \quad (10)$$

where $\text{prec}(a_t)$ denotes the preconditions of action a_t , $\text{valid}(\cdot)$ checks symbolic consistency with the domain \mathcal{D} , and λ is a weighting coefficient.

6 Experimental Setup

6.1 Data and Evaluation Metrics

We evaluate our approach on a variety of planning tasks. During evaluation, the model is prompted with the problem description alone, without additional information, prompting skills, or reasoning traces. We now provide details about the training and testing datasets.

Training Data: We have adopted the Blocksworld benchmark, with optimal solution lengths normally distributed between 0 and 20 steps (Valmeekam et al., 2023; Liang et al., 2024). **Blocks World Hard** (BW Hard) increases difficulty by extending the planning horizon, featuring solution lengths

up to 60 steps. `Blocks World Align` (`BW Align`) introduces additional actions and orientation-related requirements, with solutions up to 60 steps. We eventually obtained a training dataset size of 5807 for SFT. Full training Details are in Section A.3.1.

Testing Data: In addition to the seen task types used in training, during testing we also include unseen tasks, `Prepare Experiment`, `Reorganize Room`, and `Machine Parts Assembly`. This allows us to evaluate the model’s generalization capabilities and its transferability to real-world scenarios. These tasks require similar actions but involve more diverse objects, environments, and goals. The solution lengths are uniformly distributed between 0 and 60 steps. In total, the test set contains over 300 unseen objects and 50 furniture types, forming 1,400 novel test experiments. This design enables a thorough evaluation of the model’s ability to generalize. Further details are provided in Section A.2.1.

Evaluation Metrics: We adopt two evaluation metrics: 1) The **planning success rate** measures overall planning performance as the ratio of successfully completed tasks to the total number of tasks, following prior works (Garrett et al., 2020; Silver et al., 2023). 2) The **progress score** quantifies the similarity between the goal state and the resulting state after the first invalid action. This metric is designed to capture partial correctness, particularly in very long-horizon tasks where LLMs rarely achieve full success. The details on metric calculation are provided in Section A.2.4.

6.2 Implementation

We use the search algorithms from the Fast-Forward library (Hoffmann and Nebel, 2011), with a Python interface provided by (Garrett et al., 2020). Each training trace is defined as $\zeta^{\text{align}} = \langle \mathcal{Q}, \tau, \text{CoT}_\tau \rangle$. To prevent overfitting to narrow prompting styles, \mathcal{Q} is dynamically paraphrased by the base model during data generation (Wang et al., 2023a). The RL algorithms studied in this paper include DPO (Rafailov et al., 2023) and CPO (Achiam et al., 2017). Additional details are provided in Section A.3.

6.3 Baseline and Ablation

Baseline Models: We utilize Qwen3-4B-Instruct-2507 (denoted as Qwen3-4B) (Yang et al., 2025b) as the `SELF-CRITeach` base model. The resulting model, `SCT-4B`, is compared against the base model and other state-of-the-art LLMs of comparable scale. These include a larger variant from the Qwen3 family, Qwen3-8B, and other open-source models such as Mistral-24B, Minstral-8B (Liu et al., 2026), Gemma3-12B, Gemma3-4B (Team, 2025), as well as closed-source models such as GPT-4o (OpenAI, 2023). Details on baseline model selection and implementation are provided in Section A.2.3.

Baseline Approaches: We additionally compare our method against several reasoning-enhancement techniques for LLM-based robotic planning. These baselines include robotic knowledge distillation (Hinton et al., 2015), instantiated as self-distillation (*Self-Distill*) and teacher–student distillation (*30B-Distill*), where we distill from Qwen3-30B to Qwen3-4B. We further consider prompted chain-of-thought (*Prompt-CoT*) (Wei et al., 2022), which injects explicit reasoning prompts to guide multi-step planning, and *Majority Voting* (Wang et al., 2023b), which aggregates multiple sampled plans and selects the most consistent trajectory. All baseline approaches share the same backbone Qwen3-4B.

Ablation Studies: We conduct ablation studies to isolate the contributions of individual components in `SELF-CRITeach`. We first assess the role of symbolic-CoT transformation by comparing `SCT-4B` with `SCTSsymbol-4B`, which trains directly on symbolic traces without CoT conversion. We further evaluate variants using only supervised fine-tuning (`SCTSFT`) or only reinforcement learning (`SCTCPO`), and include Direct Preference Optimization (`SCTDPO`) (Rafailov et al., 2023) as an RL ablation. Comparisons against the full pipeline show that jointly combining symbolic-CoT transformation, SFT, and RL yields the most consistent and robust improvements.

7 Results

In this section, we present our experimental results to address the following research questions: **RQ1**. Can `SELF-CRITeach` enable a base LLM to enhance its own planning capabilities? **RQ2**. How does

the planning-enhanced model compare with similar-size SOTA models and baseline approaches? **RQ3.** Does the enhanced model demonstrate stronger performance on unseen task types? **RQ4.** Can SELF-CRITeach advance thinking efficiency?

Table 1: Planning success rate and progress score across tasks for SCT and SOTA baselines of similar size. The best results are highlighted in bold, second best are underlined. Superscripts show improvement, decline, or no change relative to SCT-4B.

Model	Seen Tasks Success Rate			Unseen Tasks Success Rate			Overall	
	BW Classic	BW Hard	BW Align	Prepare Experiment	Reorganize Room	Machine Parts Assembly	Success Rate	Progress Score
SCT-4B (ours)	0.60	0.45	0.75	0.45	0.18	0.50	0.46	0.76
Qwen3-8B	0.48 ^{-0.12}	0.28 ^{-0.17}	0.69 ^{-0.06}	0.33 ^{-0.12}	0.19 ^{+0.01}	0.40 ^{-0.1}	0.35 ^{-0.11}	0.68 ^{-0.08}
Qwen3-4B	0.41 ^{-0.19}	0.24 ^{-0.21}	0.42 ^{-0.33}	0.24 ^{-0.21}	0.12 ^{-0.06}	0.34 ^{-0.16}	0.26 ^{-0.2}	0.59 ^{-0.17}
Mistral-24B	0.21 ^{-0.39}	0.11 ^{-0.34}	<u>0.71</u> ^{-0.04}	0.18 ^{-0.27}	0.10 ^{-0.08}	0.12 ^{-0.38}	0.21 ^{-0.25}	0.49 ^{-0.27}
Minstral-8B	0.03 ^{-0.57}	0.02 ^{-0.43}	<u>0.05</u> ^{-0.7}	0.01 ^{-0.44}	0.02 ^{-0.16}	0.02 ^{-0.48}	0.02 ^{-0.44}	0.14 ^{-0.62}
Gemma3-12B	0.09 ^{-0.51}	0.08 ^{-0.37}	0.14 ^{-0.61}	0.06 ^{-0.39}	0.04 ^{-0.14}	0.11 ^{-0.39}	0.08 ^{-0.38}	0.56 ^{-0.2}
Gemma3-4B	0.01 ^{-0.59}	0.01 ^{-0.44}	0.01 ^{-0.74}	0.01 ^{-0.44}	0.01 ^{-0.17}	0.01 ^{-0.49}	0.01 ^{-0.45}	0.44 ^{-0.32}
GPT-4o	0.31 ^{-0.29}	0.17 ^{-0.28}	0.54 ^{-0.21}	0.10 ^{-0.35}	0.05 ^{-0.13}	0.11 ^{-0.39}	0.19 ^{-0.27}	0.55 ^{-0.21}

Table 2: Planning success rate and progress score across tasks for SCT and baseline approaches with Qwen3-4B as the backbone. The best results are highlighted in bold; second-best are underlined. Superscripts show improvement, decline, or no change relative to SCT-4B.

Model	Seen Tasks Success Rate			Unseen Tasks Success Rate			Overall	
	BW Classic	BW Hard	BW Align	Prepare Experiment	Reorganize Room	Machine Parts Assembly	Success Rate	Progress Score
SCT-4B (ours)	0.60	0.45	0.75	0.45	0.18	0.50	0.46	0.76
30B-Distill	0.50 ^{-0.1}	<u>0.31</u> ^{-0.14}	0.74 ^{-0.01}	0.23 ^{-0.22}	0.16 ^{-0.02}	0.49 ^{-0.01}	0.36 ^{-0.1}	0.54 ^{-0.22}
Majority Vote	0.46 ^{-0.14}	0.26 ^{-0.19}	<u>0.49</u> ^{-0.26}	<u>0.30</u> ^{-0.15}	0.15 ^{-0.03}	0.39 ^{-0.11}	0.32 ^{-0.14}	<u>0.66</u> ^{-0.1}
Self-Distill	0.45 ^{-0.15}	0.23 ^{-0.22}	0.44 ^{-0.31}	0.25 ^{-0.2}	0.13 ^{-0.05}	0.35 ^{-0.15}	0.28 ^{-0.18}	0.62 ^{-0.14}
Prompt-CoT	0.43 ^{-0.17}	0.22 ^{-0.23}	0.45 ^{-0.3}	0.24 ^{-0.21}	0.12 ^{-0.06}	0.33 ^{-0.17}	0.27 ^{-0.19}	0.64 ^{-0.12}

RQ1 Effect of Self-CriTeach The results demonstrate that SCT-4B exhibits substantially stronger planning capability than its base model, particularly in terms of generalization and long-horizon reasoning. As shown in Table 1, SCT-4B achieves consistent improvements in both overall success rate and progress score on unseen tasks, indicating enhanced robustness beyond the training distribution. SCT-4B attains a 20% absolute gain in overall success rate over the base model Qwen3-4B, with an improvement of 21% on BW Hard benchmark, highlighting its improved ability to reason over extended planning horizons. Task-specific progress scores are reported in Section A.4.

RQ2 Comparison to Other Models and Approaches. We compare SCT-4B against top-performing open-source LLM baselines of similar scale in Table 1. Despite operating at significantly smaller model scales, SCT-4B consistently outperforms all baselines. This performance advantage is especially pronounced on long-horizon tasks such as BW Hard and on unseen task distributions. A similar trend is observed when comparing alternative training and inference baselines in Table 2, indicating that SCT-4B’s gains arise from stronger planning capability rather than task-specific memorization. While some baselines achieve moderate progress scores, their low success rates reveal difficulties in maintaining global plan consistency. In contrast, SELF-CRITeach enables SCT-4B to sustain coherent long-horizon planning, resulting in more reliable task completion. Notably, we observe that more recent models exhibit stronger planning capabilities. Complete analysis is shown in Section A.4.

RQ3 Generalization Beyond improvements on seen tasks, SCT-4B demonstrates substantially stronger generalization to unseen tasks, as shown in Table 1. By reusing symbolic representations and replicating internalized planning behaviors across unseen objects, goals, and configurations, SCT-4B achieved transferable planning capabilities that scale robustly across diverse novel scenarios.

RQ4 Planning Efficiency To assess planning efficiency, we analyze the ratio between overall success rate and the average token cost per plan. All baseline approaches are included except for majority vote, whose token cost is significantly higher than others. As shown in Figure 2, SCT-4B achieves superior planning performance while maintaining higher efficiency. This improvement stems from the symbolic-CoT transformation, which provides concise supervision by eliminating reasoning steps that do not contribute to planning. Even prompting CoT to follow symbolic state transitions without

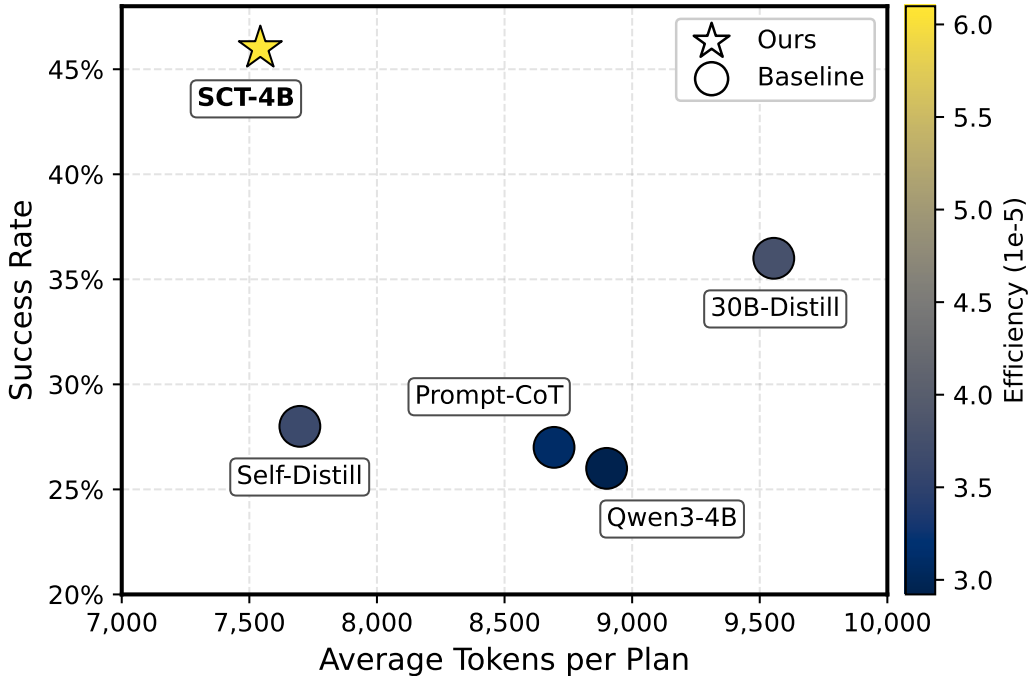


Figure 2: Overall success rate versus average per-plan token cost across top-performing baseline approaches.

Table 3: Planning success rate and progress score for SFT-only, RL-only, and symbol-only components compared to base model. The best results are highlighted in bold, second best are underlined. Superscripts show improvement, decline, or no change relative to Qwen3-4B.

Model	Seen Tasks Success Rate			Unseen Tasks Success Rate			Overall	
	BW Classic	BW Hard	BW Align	Prepare Experiment	Reorganize Room	Machine Parts Assembly	Success Rate	Progress Score
SCT-4B (ours)	0.60^{+0.19}	0.45^{+0.21}	0.75^{+0.33}	0.45^{+0.21}	0.18^{+0.06}	0.50^{+0.16}	0.46^{+0.2}	0.76^{+0.17}
SCT _{SFT} -4B	<u>0.58^{+0.17}</u>	<u>0.41^{+0.17}</u>	<u>0.67^{+0.25}</u>	<u>0.42^{+0.18}</u>	<u>0.17^{+0.05}</u>	<u>0.49^{+0.15}</u>	<u>0.43^{+0.17}</u>	<u>0.67^{+0.08}</u>
SCT _{CPO} -4B	<u>0.52^{+0.11}</u>	<u>0.33^{+0.09}</u>	<u>0.52^{+0.1}</u>	<u>0.29^{+0.05}</u>	<u>0.17^{+0.05}</u>	<u>0.35^{+0.01}</u>	<u>0.31^{+0.05}</u>	<u>0.69^{+0.1}</u>
SCT _{DPO} -4B	<u>0.47^{+0.06}</u>	<u>0.27^{+0.03}</u>	<u>0.49^{+0.07}</u>	<u>0.27^{+0.03}</u>	<u>0.16^{+0.04}</u>	<u>0.36^{+0.02}</u>	<u>0.29^{+0.03}</u>	<u>0.67^{+0.08}</u>
SCT _{Symbol} -4B	<u>0.54^{+0.13}</u>	<u>0.34^{+0.1}</u>	0.84^{+0.42}	0.16 ^{-0.08}	<u>0.14^{+0.02}</u>	0.50^{+0.16}	<u>0.38^{+0.12}</u>	<u>0.62^{+0.03}</u>
Qwen3-4B	0.41	0.24	0.42	0.24	0.12	0.34	0.26	0.59

training already slightly reduces token cost. Notably, SCT-4B outperforms 30B-Distill, indicating that symbolic-CoT supervision offers higher-quality training signals than distilling from large reasoning models. A detailed analysis is provided in Section A.4.

8 Ablation Study

In this section, we present ablation studies of SELF-CRITeach to address the following research question. **RQ5.** What roles do the three components, SFT, RL, and symbolic-CoT, play in SELF-CRITeach?

RQ5 Roles of Components in SELF-CRITeach. As is shown in Table 3, using the self-generated planning domain for either SFT or RL alone already significantly improves over the base model. SFT yields substantial gains in progress score across both seen and unseen tasks, indicating that symbolic-CoT supervision provides a strong inductive bias for structured planning. Combining SFT with RL further improves both progress score and success rate; the larger improvement margin in progress score indicates a substantial reduction in state-transition violations, showing that CPO complements SFT by reinforcing constraint satisfaction. Among RL variants, CPO consistently outperforms DPO, likely due to CPO’s explicit constraint enforcement, which better aligns with

Table 4: Real-robot task success rates comparison between SCT-4B and PDDL-planner under different perception methods.

Logical States Estimation	SCT-4B		PDDL Solver	
	Room	Lab	Room	Lab
Qwen3-VL-4B	0.70	0.60	0.40	0.20
Rule-based Classifier	0.80	0.90	0.70	0.70

the step-wise feasibility checks of symbolic planning. Finally, directly training the base model on symbolic plans without CoT transformation exhibits unstable generalization despite improvements on seen tasks, suggesting a tendency of solution memorization rather than true internalization of planning structure and highlighting the importance of symbolic-CoT transformation to achieve transferable and generalizable planning.

9 Real Robot Experiment

PDDL-based task planners are brittle under incomplete or noisy logical states from imperfect perception. Motivated by this limitation, we conduct two real-robot experiments to evaluate the real-world compatibility of SCT-4B and compare it against a PDDL solver, shown in Figure 3. We deploy SCT-4B on a real UR5e robot using the UR5e control API as low-level skills, and evaluate two tasks—Reorganize Room (Room) and Prepare WetLab Experiment with water-bath heating (Lab)—under two perception pipelines: (1) ground-truth poses with a rule-based classifier, and (2) a VLM, Qwen3-VL-4B (Bai et al., 2025) to directly predict logical states. Ten trials are performed for each task.

The results in Table 4 demonstrate SCT-4B’s improved resistance to imperfect logical state. Both VLMs and rule-based classifiers introduce noise: VLMs are affected by partial observability, spatial reasoning errors, and transparent-object detection, while rule-based classifiers fail in edge cases and nested relations, leading to missing or inconsistent predicates. Under such noisy logical states, PDDL solvers are brittle and prone to failure. In contrast, SCT-4B can reason over and plan with partial

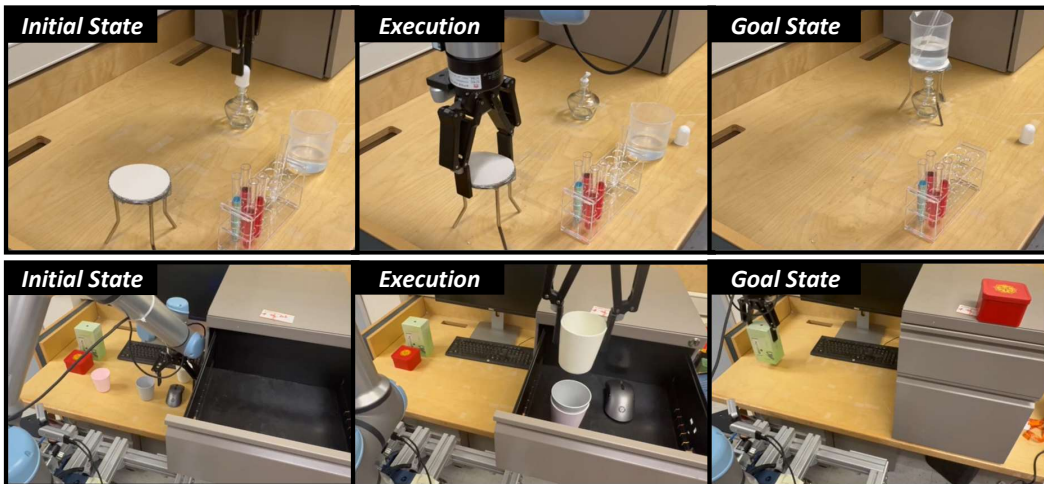


Figure 3: Real Robot Planning with SCT-4B: Reorganize Room (Lower, 13 steps) ; Prepare Experiment (Upper, 8 steps)

symbolic observations despite state estimation errors. These experiments highlight the superior deployability of SCT-4B on real robots and its compatibility with practical perception and control pipelines.

10 Limitations & Future Work

While SELF-CRITEACH demonstrates strong improvements in planning, several limitations remain. First, the framework assumes the base LLM has sufficient reasoning capability to induce coherent PDDL planning domains. Second, it assumes that target tasks can be accurately modeled in a symbolic space, which may not hold for tasks with complex continuous constraints. Future work will explore planning-domain generation methods with lower requirements on base model capability, improved symbolic abstraction for perceptually complex tasks, and more adaptive skill discovery and online learning during real-robot execution.

11 Conclusion

In this work, we introduce SELF-CRITEACH, a self-teaching and self-critiquing framework that leverages LLM-generated planning domains as scalable sources of verified supervision and structured reward signals. By treating planning domains as data engines, SELF-CRITEACH automatically constructs diverse long-horizon task plans that surpass the base model’s intrinsic planning ability without human curation. Through symbolic-to-CoT transformation, the framework bridges formal symbolic structures with natural-language reasoning, enabling models to internalize search behavior and planning skills. RL post-training with the planning domain as rewards further refines planning under structured constraints. Empirically, SELF-CRITEACH yields substantial gains in planning success, generalization, and token efficiency, and maintains robustness to imperfect logical states during real-robot execution, demonstrating practical applicability to realistic robotic systems.

References

Joshua Achiam, David Held, Aviv Tamar, and Pieter Abbeel. 2017. CPO: Constrained Policy Optimization. In Proc. Int. Conf. on Machine Learning (ICML).

Ashay Athalye, Nishanth Kumar, Tom Silver, Yichao Liang, Jiuguang Wang, Tomás Lozano-Pérez, and Leslie Pack Kaelbling. 2024. From Pixels to Predicates: Learning Symbolic World Models via Pretrained Vision-Language Models. arXiv preprint arXiv:2501.00296 (2024).

Shuai Bai, Yuxuan Cai, Ruizhe Chen, Keqin Chen, Xionghui Chen, Zesen Cheng, Lianghao Deng, Wei Ding, Chang Gao, Chunjiang Ge, Wenbin Ge, Zhifang Guo, Qidong Huang, Jie Huang, Fei Huang, Binyuan Hui, Shutong Jiang, Zhaohai Li, Mingsheng Li, Mei Li, Kaixin Li, Zicheng Lin, and et al. 2025. Qwen3-VL Technical Report. arXiv preprint arXiv:2511.21631 (2025).

Kevin Black, Noah Brown, Danny Driess, Adnan Esmail, Michael Equi, Chelsea Finn, Niccolò Fusai, Lachy Groom, Karol Hausman, Brian Ichter, Szymon Jakubczak, Tim Jones, Liyiming Ke, Sergey Levine, Adrian Li-Bell, Mohith Mothukuri, Suraj Nair, Karl Pertsch, Lucy Xiaoyang Shi, James Tanner, Quan Vuong, Anna Walling, Haohuan Wang, and Ury Zhilinsky. 2024. π_0 : A vision-language-action flow model for general robot control. arXiv preprint arXiv:2410.24164 (2024).

Anthony Brohan, Yevgen Chebotar, Chelsea Finn, Karol Hausman, Alexander Herzog, Daniel Ho, Julian Ibarz, Alex Irpan, Eric Jang, Ryan Julian, et al. 2022. Do as i can, not as i say: Grounding language in robotic affordances. In Proc. Conf. on Robot Learning.

Tom Brown, Benjamin Mann, Nick Ryder, Melanie Subbiah, Jared D Kaplan, Prafulla Dhariwal, Arvind Neelakantan, Pranav Shyam, Girish Sastry, Amanda Askell, Sandhini Agarwal, Ariel Herbert-Voss, Gretchen Krueger, et al. 2020. Language Models are Few-Shot Learners. In Proc. Adv. Neural Inf. Proc. Systems.

Walker Byrnes, Miroslav Bogdanovic, Avi Balakirsky, Stephen Balakirsky, and Animesh Garg. 2024. CLIMB: Language-guided continual learning for task planning with iterative model building. arXiv [cs.RO] (2024).

Yongchao Chen, Jacob Arkin, Yilun Hao, Yang Zhang, Nicholas Roy, and Chuchu Fan. 2024. PRompt Optimization in Multi-Step Tasks (PROMST): Integrating Human Feedback and Heuristic-based Sampling. In Proc. Conf. Empirical Methods in Natural Language Processing.

Yongchao Chen, Jacob Arkin, Yang Zhang, Nicholas A. Roy, and Chuchu Fan. 2023. AutoTAMP: Autoregressive Task and Motion Planning with LLMs as Translators and Checkers. In Proc. IEEE Int. Conf. on Robotics and Automation.

Paul F Christiano, Jan Leike, Tom Brown, Miljan Martic, Shane Legg, and Dario Amodei. 2017. Deep Reinforcement Learning from Human Preferences. In Advances in Neural Information Processing Systems, Vol. 30. Curran Associates, Inc.

Karl Cobbe, Vineet Kosaraju, Mohammad Bavarian, Mark Chen, Heewoo Jun, Lukasz Kaiser, Matthias Plappert, Jerry Tworek, Jacob Hilton, Reiichiro Nakano, et al. 2021. Training Verifiers to Solve Math Word Problems. In arXiv preprint arXiv:2110.14168.

Murtaza Dalal, Ajay Mandlekar, Caelan Reed Garrett, Ankur Handa, Ruslan Salakhutdinov, and Dieter Fox. 2023. Imitating Task and Motion Planning with Visuomotor Transformers. In Proceedings of The 7th Conference on Robot Learning. 2565–2593.

Maximilian Diehl, Chris Paxton, and Karinne Ramirez-Amaro. 2021. Automated Generation of Robotic Planning Domains from Observations. 2021 IEEE/RSJ International Conference on Intelligent Robots and Systems (IROS) (2021).

Danny Driess, F Xia, Mehdi S M Sajjadi, Corey Lynch, Aakanksha Chowdhery, Brian Ichter, Ayzaan Wahid, Jonathan Tompson, Q Vuong, Tianhe Yu, Wenlong Huang, Yevgen Chebotar, P Sermanet, Daniel Duckworth, S Levine, Vincent Vanhoucke, Karol Hausman, Marc Toussaint, Klaus Greff, Andy Zeng, Igor Mordatch, and Peter R Florence. 2023. PaLM-E: An embodied multimodal language model. In Proc. Int. Conf. on Machine Learning.

Jiazhan Feng, Ruochen Xu, Junheng Hao, Hiteshi Sharma, Yelong Shen, Dongyan Zhao, and Weizhu Chen. 2024. Language Models can be Deductive Solvers. In Findings of the Association for Computational Linguistics: NAACL 2024.

Caelan Reed Garrett, Tomás Lozano-Pérez, and Leslie Pack Kaelbling. 2020. PDDLStream: Integrating symbolic planners and blackbox samplers via optimistic adaptive planning. Proc. Int. Conf. Autom. Plan. Sched. (2020).

Lin Guan, Karthik Valmecikam, Sarath Sreedharan, and Subbarao Kambhampati. 2023. Leveraging Pre-trained Large Language Models to Construct and Utilize World Models for Model-based Task Planning. In Proc. Adv. Neural Inf. Proc. Systems.

Abhishek Gupta, Vikash Kumar, Corey Lynch, Sergey Levine, and Karol Hausman. 2019. Relay Policy Learning: Solving Long Horizon Tasks via Imitation and Reinforcement Learning. Conference on Robot Learning (CoRL) (2019).

Muzhi Han, Yifeng Zhu, Song-Chun Zhu, Ying Nian Wu, and Yuke Zhu. 2024b. InterPreT: Interactive Predicate Learning from Language Feedback for Generalizable Task Planning. In Robotics: Science and Systems (RSS).

Simeng Han, Hailey Schoelkopf, Yilun Zhao, Zhenting Qi, Martin Riddell, Wenfei Zhou, James Coady, David Peng, Yujie Qiao, Luke Benson, Lucy Sun, Alexander Wardle-Solano, Hannah Szabó, Ekaterina Zubova, Matthew Burtell, Jonathan Fan, Yixin Liu, Brian Wong, Malcolm Sailor, Ansong Ni, Linyong Nan, Jungo Kasai, Tao Yu, Rui Zhang, Alexander Fabbri, Wojciech Maciej Kryscinski, Semih Yavuz, Ye Liu, Xi Victoria Lin, Shafiq Joty, Yingbo Zhou, Caiming Xiong, Rex Ying, Arman Cohan, and Dragomir Radev. 2024a. FOLIO: Natural Language Reasoning with First-Order Logic. In Proceedings of the 2024 Conference on Empirical Methods in Natural Language Processing.

Geoffrey Hinton, Oriol Vinyals, and Jeff Dean. 2015. Distilling the knowledge in a neural network. arXiv preprint arXiv:1503.02531 (March 2015).

J Hoffmann and B Nebel. 2011. The FF planning system: Fast plan generation through heuristic search. arXiv [cs.AI] (June 2011).

Arian Hosseini, Xingdi Yuan, Nikolay Malkin, Aaron Courville, Alessandro Sordoni, and Rishabh Agarwal. 2024. V-STaR: Training verifiers for self-taught reasoners. In Proceedings of the 2024 Conference on Language Modeling.

Mengkang Hu, Yao Mu, Xinmiao Yu, Mingyu Ding, Shiguang Wu, Wenqi Shao, Qiguang Chen, Bin Wang, Yu Qiao, and Ping Luo. 2023. Tree-Planner: Efficient close-loop task planning with Large Language Models. arXiv preprint arXiv:2310.08582 (2023).

Jinbang Huang, Allen Tao, Rozilyn Marco, Miroslav Bogdanovic, Jonathan Kelly, and Florian Shkurti. 2025a. Automated Planning Domain Inference for Task and Motion Planning. In 2025 IEEE International Conference on Robotics and Automation (ICRA). IEEE, 12534–12540.

Jinbang Huang, Yixin Xiao, Zhanguang Zhang, Mark Coates, Jianye Hao, and Yingxue Zhang. 2025b. One demo is all it takes: Planning Domain Derivation with LLMs from A single demonstration. arXiv preprint at arXiv:2505.18382 (May 2025).

Wenlong Huang, Pieter Abbeel, Deepak Pathak, and Igor Mordatch. 2022a. Language Models as Zero-Shot Planners: Extracting Actionable Knowledge for Embodied Agents. In Proc. Int. Conf. on Machine Learning.

Wenlong Huang, Fei Xia, Ted Xiao, Harris Chan, Jacky Liang, Pete Florence, Andy Zeng, Jonathan Tompson, Igor Mordatch, Yevgen Chebotar, Pierre Sermanet, Tomas Jackson, Noah Brown, Linda Luu, Sergey Levine, Karol Hausman, and Brian Ichter. 2022b. Inner Monologue: Embodied Reasoning through Planning with Language Models. In Proc. Conf. on Robot Learning.

Mohamed Khodeir, Ben Agro, and Florian Shkurti. 2023. Learning to Search in Task and Motion Planning With Streams. IEEE Robotics and Automation Letters (2023).

Takeshi Kojima, Shixiang (Shane) Gu, Machel Reid, Yutaka Matsuo, and Yusuke Iwasawa. 2022. Large Language Models are Zero-Shot Reasoners. In Proc. Adv. Neural Inf. Proc. Systems.

Tejas D Kulkarni, Karthik Narasimhan, Ardavan Saeedi, and Josh Tenenbaum. 2016. Hierarchical Deep Reinforcement Learning: Integrating Temporal Abstraction and Intrinsic Motivation. In Advances in Neural Information Processing Systems, Vol. 29. Curran Associates, Inc.

Nishanth Kumar, Willie McClinton, Rohan Chitnis, Tom Silver, Tomás Lozano-Pérez, and Leslie Pack Kaelbling. 2023. Learning Efficient Abstract Planning Models that Choose What to Predict. In Proc. Conf. on Robot Learning.

Jaehyeok Lee, Keisuke Sakaguchi, and Jinyeong Bak. 2025. Self-training meets consistency: Improving LLMs' reasoning with consistency-driven rationale evaluation. In Proceedings of the 2025 Conference of the Nations of the Americas Chapter of the Association for Computational Linguistics: Human Language Technologies (Volume 1: Long Papers).

Boyi Li, Philipp Wu, Pieter Abbeel, and Jitendra Malik. 2023. Interactive Task Planning with Language Models. In Proc. 2nd Workshop on Language and Robot Learning.

Yichao Liang, Nishanth Kumar, Hao Tang, Adrian Weller, Joshua B Tenenbaum, Tom Silver, João F Henriques, and Kevin Ellis. 2024. VisualPredicator: Learning abstract world models with Neuro-Symbolic Predicates for robot planning. arXiv preprint arXiv:2410.23156 (2024).

Alexander H. Liu, Kartik Khandelwal, Sandeep Subramanian, Victor Jouault, Abhinav Rastogi, Adrien Sadé, Alan Jeffares, Albert Jiang, Alexandre Cahill, Alexandre Gavaudan, Alexandre Sablayrolles, Amélie Héliou, Amos You, Andy Ehrenberg, Andy Lo, Anton Eliseev, and et al. 2026. Ministral 3. arXiv preprint arXiv:2601.08584 (2026). Introduces the Ministral 3 series of models (3B, 8B, 14B) and their instruct finetuned variants.

Bo Liu, Yuqian Jiang, Xiaohan Zhang, Qiang Liu, Shiqi Zhang, Joydeep Biswas, and Peter Stone. 2023. LLM+P: Empowering large language models with optimal planning proficiency. arXiv preprint arXiv:2304.11477 (2023).

Weiyu Liu, Neil Nie, Ruohan Zhang, Jiayuan Mao, and Jiajun Wu. 2024. Learning Compositional Behaviors from Demonstration and Language. In Proceedings of The 8th Conference on Robot Learning.

Drew McDermott, Malik Ghallab, Adele E. Howe, Craig A. Knoblock, Ashwin Ram, Manuela M. Veloso, Daniel S. Weld, and David E. Wilkins. 1998. PDDL-the planning domain definition language.

Silin Meng, Yiwei Wang, Cheng-Fu Yang, Nanyun Peng, and Kai-Wei Chang. 2024. LLM-A*: Large Language Model Enhanced Incremental Heuristic Search on Path Planning. In Findings of the Assoc. for Comput. Linguistics: EMNLP 2024.

Theo Olausson, Alex Gu, Ben Lipkin, Cedegao Zhang, Armando Solar-Lezama, Joshua Tenenbaum, and Roger Levy. 2023. LINC: A Neurosymbolic Approach for Logical Reasoning by Combining Language Models with First-Order Logic Provers. In Proceedings of the 2023 Conference on Empirical Methods in Natural Language Processing.

OpenAI. 2023. GPT-4 Technical Report. arXiv preprint arXiv:2303.08774 (2023).

James Oswald, Kavitha Srinivas, Harsha Kokel, Junkyu Lee, Michael Katz, and Shirin Sohrabi. 2024. Large language models as planning domain generators. In Proc. Int. Conf. on Automated Planning and Scheduling.

Long Ouyang, Jeff Wu, Xu Jiang, Diogo Almeida, Carroll Wainwright, Pamela Mishkin, Chong Zhang, Sandhini Agarwal, Katarina Slama, Alex Ray, et al. 2022. Training Language Models to Follow Instructions with Human Feedback. In Proc. Adv. Neural Inf. Proc. Systems.

Jiayi Pan, Glen Chou, and Dmitry Berenson. 2023b. Data-Efficient Learning of Natural Language to Linear Temporal Logic Translators for Robot Task Specification. In Proceedings of the 2023 IEEE International Conference on Robotics and Automation (ICRA).

Liangming Pan, Alon Albalak, Xinyi Wang, and William Yang Wang. 2023a. Logic-LM: Empowering Large Language Models with Symbolic Solvers for Faithful Logical Reasoning. In The 2023 Conference on Empirical Methods in Natural Language Processing.

Rafael Rafailov, Archit Sharma, Eric Mitchell, Stefano Ermon, Christopher D. Manning, and Chelsea Finn. 2023. Direct preference optimization: your language model is secretly a reward model. In Proceedings of the 37th International Conference on Neural Information Processing Systems (New Orleans, LA, USA) (NIPS '23). Curran Associates Inc., Red Hook, NY, USA, Article 2338, 14 pages.

John Schulman, Filip Wolski, Prafulla Dhariwal, Alec Radford, and Oleg Klimov. 2017. Proximal Policy Optimization Algorithms. arXiv [cs.LG] (July 2017).

Pierre Sermanet, Tianli Ding, Jeffrey Zhao, Fei Xia, Debidatta Dwibedi, Keerthana Gopalakrishnan, Christine Chan, Gabriel Dulac-Arnold, Sharath Maddineni, Nikhil J. Joshi, Pete Florence, Wei Han, Robert Baruch, Yao Lu, Suvir Mirchandani, Peng Xu, Pannag R. Sanketi, Karol Hausman, Izhak Shafran, Brian Ichter, and Yuan Cao. 2023. RoboVQA: Multimodal Long-Horizon Reasoning for Robotics. Proc. IEEE Int. Conf. on Robotics and Automation (2023).

Zhihong Shao, Peiyi Wang, Qihao Zhu, Runxin Xu, Junxiao Song, Mingchuan Zhang, Y K Li, Y Wu, and Daya Guo. 2024. DeepSeekMath: Pushing the limits of mathematical reasoning in open language models. arXiv [cs.CL] (Feb. 2024).

Tom Silver, Rohan Chitnis, Nishanth Kumar, Willie McClinton, Tomás Lozano-Pérez, Leslie Kaelbling, and Joshua B Tenenbaum. 2023. Predicate Invention for Bilevel Planning. In Proc. AAAI Conf. on Artificial Intelligence.

Tom Silver, Soham Dan, Kavitha Srinivas, Joshua B Tenenbaum, Leslie Kaelbling, and Michael Katz. 2024. Generalized planning in pddl domains with pretrained large language models. In Proc. AAAI Conf. on Artificial Intelligence.

Kaya Stechly, Karthik Valmeekam, and Subbarao Kambhampati. 2024. Chain of Thoughtlessness? An Analysis of CoT in Planning. In Proc. Adv. Neural Inf. Proc. Systems.

Oyvind Tafjord, Bhavana Dalvi, and Peter Clark. 2021. ProofWriter: Generating Implications, Proofs, and Abductive Statements over Natural Language. In Findings of the Association for Computational Linguistics: ACL-IJCNLP 2021.

Gemma Team. 2025. Gemma 3 Technical Report. arXiv preprint arXiv:2503.19786 (2025).

Yuxuan Tong, Xiwen Zhang, Rui Wang, Ruidong Wu, and Junxian He. 2024. DART-Math: Difficulty-Aware Rejection Tuning for Mathematical Reasoning. In Proc. Adv. Neural Inf. Proc. Systems.

Karthik Valmeekam, Matthew Marquez, Alberto Olmo, Sarath Sreedharan, and Subbarao Kambhampati. 2023. PlanBench: an extensible benchmark for evaluating large language models on planning and reasoning about change. In Proc. Adv. Neural Inf. Proc. Systems.

Shu Wang, Muzhi Han, Ziyuan Jiao, Zeyu Zhang, Yingnian Wu, Song-Chun Zhu, and Hangxin Liu. 2024. LLM3: Large Language Model-based Task and Motion Planning with Motion Failure Reasoning. In Proc. IEEE/RSJ Int. Conf. on Intelligent Robots and Systems.

Xuezhi Wang, Jason Wei, Dale Schuurmans, Quoc V Le, Ed H. Chi, Sharan Narang, Aakanksha Chowdhery, and Denny Zhou. 2023b. Self-Consistency Improves Chain of Thought Reasoning in Language Models. In International Conference on Learning Representations (ICLR).

Yile Wang, Sijie Cheng, Zixin Sun, Peng Li, and Yang Liu. 2025a. Leveraging Language-based Representations for Better Solving Symbol-related Problems with Large Language Models. In Proceedings of the 31st International Conference on Computational Linguistics.

Yizhong Wang, Yeganeh Kordi, Swaroop Mishra, Alisa Liu, Noah A. Smith, Daniel Khashabi, and Hannaneh Hajishirzi. 2023a. Self-Instruct: Aligning Language Models with Self-Generated Instructions. In Proceedings of the 61st Annual Meeting of the Association for Computational Linguistics (Volume 1: Long Papers).

Yuyao Wang, Bowen Liu, Jianheng Tang, Nuo Chen, Yuhan Li, Qifan Zhang, and Jia Li. 2025b. Graph-R1: Unleashing LLM Reasoning with NP-Hard Graph Problems. [arXiv preprint arXiv:2508.20373](#) (2025).

Jason Wei, Xuezhi Wang, Dale Schuurmans, Maarten Bosma, Brian Ichter, Fei Xia, Ed H. Chi, Quoc V. Le, and Denny Zhou. 2022. Chain-of-thought prompting elicits reasoning in large language models. In [Proc. Adv. Neural Inf. Proc. Systems](#).

Lionel Wong, Jiayuan Mao, Pratyusha Sharma, Zachary S Siegel, Jiahai Feng, Noa Korneev, Joshua B Tenenbaum, and Jacob Andreas. 2023. Learning adaptive planning representations with natural language guidance. [arXiv \[cs.AI\]](#) (2023).

Jundong Xu, Hao Fei, Liangming Pan, Qian Liu, Mong Li Lee, and Wynne Hsu. 2024. Faithful Logical Reasoning via Symbolic Chain-of-Thought. In [Annual Meeting of the Association for Computational Linguistics](#).

An Yang, Anfeng Li, Baosong Yang, Beichen Zhang, Binyuan Hui, Bo Zheng, Bowen Yu, Chang Gao, Chengen Huang, Chenxu Lv, Chujie Zheng, Dayiheng Liu, Fan Zhou, Fei Huang, Feng Hu, Hao Ge, Haoran Wei, Huan Lin, Jialong Tang, Jian Yang, Jianhong Tu, Jianwei Zhang, Jianxin Yang, Jiaxi Yang, Jing Zhou, Jingren Zhou, Junyang Lin, Kai Dang, Keqin Bao, Kexin Yang, Le Yu, Lianghao Deng, Mei Li, Mingfeng Xue, Mingze Li, Pei Zhang, Peng Wang, Qin Zhu, Rui Men, Ruize Gao, Shixuan Liu, Shuang Luo, Tianhao Li, Tianyi Tang, Wenbiao Yin, Xingzhang Ren, Xinyu Wang, Xinyu Zhang, Xuancheng Ren, Yang Fan, Yang Su, Yichang Zhang, Yinger Zhang, Yu Wan, Yuqiong Liu, Zekun Wang, Zeyu Cui, Zhenru Zhang, Zhipeng Zhou, and Zihan Qiu. 2025b. Qwen3 Technical Report. [arXiv preprint arXiv:2505.09388](#) (2025).

Zhutian Yang, Caelan Garrett, Dieter Fox, Tomás Lozano-Pérez, and Leslie Pack Kaelbling. 2025a. Guiding Long-Horizon Task and Motion Planning with Vision Language Models. In [2025 IEEE International Conference on Robotics and Automation \(ICRA\)](#). 16847–16853.

Shunyu Yao, Dian Yu, Jeffrey Zhao, Izhak Shafran, Thomas L. Griffiths, Yuan Cao, and Karthik R Narasimhan. 2023. Tree of Thoughts: Deliberate Problem Solving with Large Language Models. In [Proc. Adv. Neural Inf. Proc. Systems](#).

Zheng Yuan, Hongyi Yuan, Chengpeng Li, Guanting Dong, Keming Lu, Chuanqi Tan, Chang Zhou, and Jingren Zhou. 2023. Scaling Relationship on Learning Mathematical Reasoning with Large Language Models. [arXiv preprint arXiv:2308.01825](#) (2023).

Eric Zelikman, Yuhuai Wu, Jesse Mu, and Noah D. Goodman. 2022. STaR: self-taught reasoner bootstrapping reasoning with reasoning. In [Proc. Adv. Neural Inf. Proc. Systems](#).

Zirui Zhao, Wee Sun Lee, and David Hsu. 2024. Large language models as commonsense knowledge for large-scale task planning. In [Proc. Adv. Neural Inf. Proc. Systems](#).

Wang Zhu, Ishika Singh, Robin Jia, and Jesse Thomason. 2024. Language Models can infer action semantics for symbolic planners from environment feedback. [arXiv \[cs.AI\]](#) (2024).

A Appendix

A.1 LLM-based Domain Generation

A.1.1 Initial Domain Skeleton Construction

The first stage of SELF-CRITeach is the automatic construction of symbolic planning domains. We leverage the generative capacity of the base model \mathcal{M}_0 to propose candidate predicates that capture object relations and intrinsic properties, guided by physical simulation. The overall pipeline follows the domain generation framework proposed by Huang et al. (2025b). Input \mathcal{U} is a demonstration trajectory with a short task description. Subsequently, we prompt \mathcal{M}_0 with demonstration trajectories collected by the Agilex Pika Data Collection System to invent actions, which are then compiled into executable planning domains. The model outputs a preliminary PDDL domain skeleton $\mathcal{D}_0 = \langle \mathcal{P}, \mathcal{A} \rangle$, where \mathcal{P} denotes the set of predicates and \mathcal{A} the set of actions with preconditions and effects. This skeleton is then tested against a suite of sampled planning problems $\{\mathcal{Q}_i\}$ using the Fast-Forward planner (Hoffmann and Nebel, 2011; Garrett et al., 2020). Successful execution indicates a consistent domain; otherwise, domain errors are detected and used for refinement.

A.1.2 Feedback-Driven Planning Domain Repair

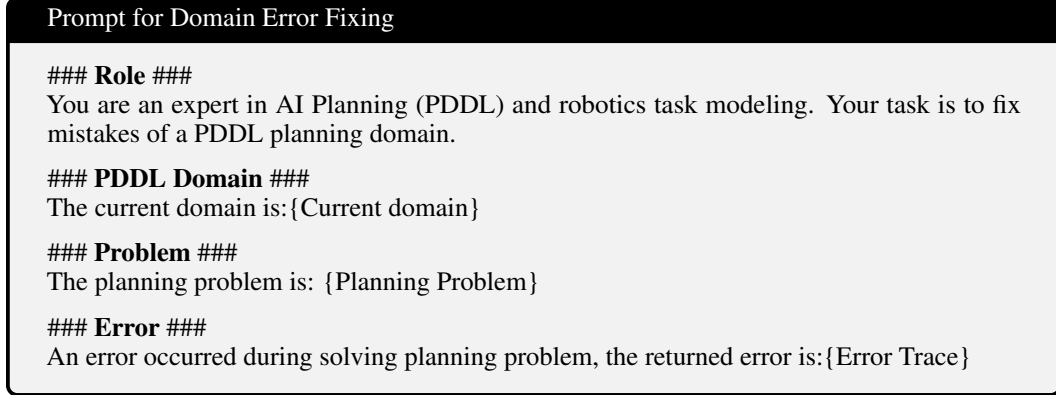
When validation fails, SELF-CRITeach introduces two complementary self-correction mechanisms.

Feedback prompting. Error traces from the planner (e.g., undefined predicate) are reformulated into feedback prompts. These prompts are re-injected into \mathcal{M}_0 to request targeted corrections, following the iterative refinement proposed in (Guan et al., 2023; Oswald et al., 2024).

Formally, given error e produced on problem \mathcal{Q}_i , we define a feedback function

$$h(e, \mathcal{Q}_i) \rightarrow \text{diagnostic prompt } d,$$

which is appended to the domain-fix query to produce a repaired domain \mathcal{D}_{t+1} . This iteration is repeated until a consistent and executable domain \mathcal{D}' is generated. Prompt Template is as following:



Hill-Climbing Search for Domain Redundancy Pruning In addition to error repair, generated domains often contain redundant predicates and actions. To address this, we employ a symbolic hill-climbing algorithm (Silver et al., 2023; Kumar et al., 2023; Huang et al., 2025a) that prunes unnecessary components from the domain. This procedure ensures that the final domain \mathcal{D}^* is both executable and minimal, containing only semantically necessary components.

A.1.3 Automatic Problem–Plan Pair Generation

Once a validated domain \mathcal{D}^* is obtained, we generate a library of problem–plan pairs (\mathcal{Q}, τ) . Each problem is constructed by sampling initial and goal states consistent with \mathcal{D}^* , and solved with the symbolic planner. The resulting pairs are later aligned with chain-of-thought explanations to form the training traces used in SELF-CRITeach.

A.2 Evaluation Details

A.2.1 Evaluation Data Details

The evaluation dataset consists of seven disjoint task datasets: *stack-200*, *unstack-200*, *reorder-200*, and *align-200* (Blocks World domain), along with *prepare-experiment-200*, *reorganize-room-200*, and *machine-parts-assembly-200*. Each dataset comprises 200 tasks, with solution lengths uniformly sampled across four intervals: 0–10, 10–20, 20–30, and 30+ steps.

Next, we discuss how each testing set is augmented and the detailed difficulty distribution:

Seen Tasks:

- *Blocks World-Classic* is a reproduction of the traditional Blocks World benchmark, consisting of 100 problem instances across the stack, unstack, and reorder tasks. The optimal plan lengths approximately follow a normal distribution within 0–20 steps. The details of test problem distribution of Blocks World Classic are shown in Figure 4
- *Blocks World-Hard* extends the benchmark to include more challenging problems with longer optimal plan lengths up to 60 steps. The distribution of problem counts across four difficulty intervals is kept balanced. It contains 200 problem instances for each of the three task types: stack, unstack, and reorder.
- *Blocks World-Align* further extends the benchmark by introducing orientation reasoning. In addition to the standard actions, a rotate action is included, requiring the model to reason about spatial orientations.

Unseen Tasks

- *Reorganize Room*: The robot must collect household items, redistribute them to their designated locations, and pack them according to specified requirements.
- *Machine Parts Assembly*: The robot must collect machining parts distributed across the factory and assemble them in the required order.
- *Prepare Experiment*: The robot must retrieve laboratory equipment and set up an experimental platform.

The unseen tasks include a large scale diverse objects (over 300) and furniture (over 50), the details are shown in the following section.

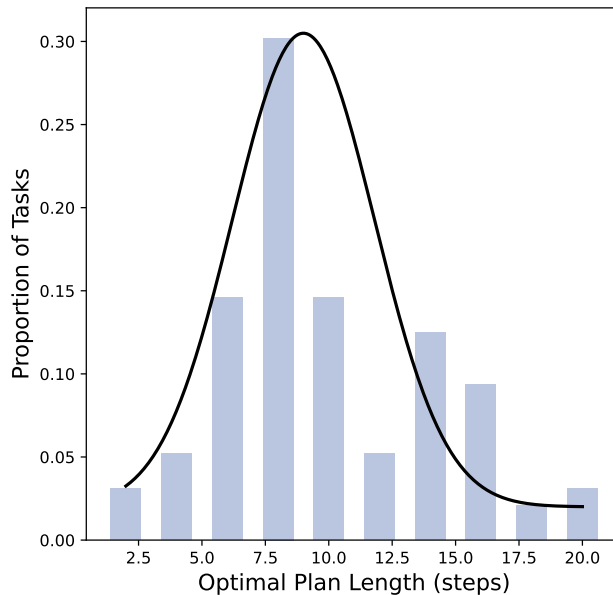


Figure 4: Evaluation data distribution for Blocks World Classic

A.2.2 Unseen Object Types and Furniture Included in Test Set

HouseKeeping Objects

shoebox, book, towel, cushion, pillow, blanket, toyblock, jar, canister, bin, basket, tilepack, box, storagebox, detergent, soapbar, tissuebox, magazine, photoalbum, cuttingboard, foodbox, ricebag, flourbag, sugarbag, spicejar, candle, cup, plate, pot, pan, tray, bucket, stepbox, organizer, toybox, craftbox, sewingbox, pillowbox, laundrybox, clothbag, storagecrate, hamper, cushionbox, shelfbox, matpack, drivecase, clipboard, penbox, pencilbox, markerbox, staplebox, tape, tapeholder, calendar, planner, report, documentbox, letterbox, envelopebox, badgebox, tagbox, cardbox, stampbox, inkpad, paperroll, chartbook, whiteboard, pinboard, notepad, scrapbook, catalog, supplybox, lunchbox, laptopbox, headsetcase, monitorbox, keyboardbox, mousebox, cablebox, dockbox, shoes, slippers, sandals, boots, books, magazines, notebooks, comics, albums, photoalbums, towels, napkins, blankets, pillows, cushions, plates, bowls, cups, glasses, mugs, cutlery, forks, spoons, knives, chopsticks, spicejars, condiments, cerealboxes, snackpacks, bottles, jars, cans, storagebins, shoeboxes, laundrybaskets, soapbars, detergents, shampoos, conditioners, lotions, toothbrushes, toothpastes, razors, combs, brushes, hats, scarves, belts, ties, gloves

Factory Objects

pallet, crate, ingot, brick, block, mold, drum, barrel, tray, spool, battery, foam, plate, rod, beam, sheet, coil, carton, gearbox, motor, casing, bearingbox, brickpack, cablebox, metalbox, plasticbin, boltpail, nutbox, washerbox, pipebundle, timber, lumber, steelbar, rebar, partbox, panel, duct, filterbox, container, powderbag, sack, clampbox, toolkit, spacerblock, fastenerbox, weldrod, fixture, drillbox, pallets, crates, bricks, blocks, beams, pipes, rods, bars, rebars, sheets, panels, plates, coils, rolls, cylinders, drums, barrels, containers, boxes, cartons, bolts, nuts, washers, screws, clamps, wrenches, spanners, drills, toolbits, sockets, filters, gaskets, valves, hoses, cables, chains, belts, wheels, gears, motors, casings, bearings, molds, fixtures, frames, foampads, straps, seals, packaging, labels

Lab Objects

rack, cylinder, labbox, carton, container, samplebox, tipbox, cryobox, pack, dish, slidebox, capsule, pouch, filterbox, tray, case, testbox, bufferbox, kit, bag, tubecrate, platebox, medium-bottle, sealbag, gelbox, reagentbox, chipbox, cellbox, rackbox, capbox, powderjar, acidbottle, solventcan, stockbottle, samplejar, drybox, packtube, enzymebox, coolerbox, chemcart, bottles, beakers, flasks, cylinders, vials, tubes, testtubes, petri, slides, racks, tipboxes, cryoboxes, samplebags, pipettes, pipettips, dishes, capsules, ampoules, filters, funnels, gloves, masks, goggles, aprons, coats, notebooks, pens, labels, markers, tags, trays, cases, carts, stands, supports, boxes, containers, jars, pouches, packs, media, solutions, buffers, reagents, kits, cells, chips, plates, serums, enzymes

Housekeeping Furniture

dining table, coffee table, side table, console table, end table, bedside table, kitchen table, foldable table, picnic table, patio table, round table, square table, rectangular table, buffet table, sofa table, low table, tea table, serving table, bench table, counter table, island table, tv stand, hall table, display table, exhibit table, study desk, writing desk, computer desk, standing desk, reception desk, conference table, meeting table, office table, printer stand, workstation, drafting table, blueprint table

Factory Furniture

workbench, assembly table, packing table, utility table, sorting table, assembly bench, grinding table

Lab Furniture

lab bench, lab table, specimen table, experiment bench, fume table, inspection table

A.2.3 Evaluation Implementation Details

We built a unified evaluation pipeline for all experiments. The pipeline loads each evaluation dataset and constructs prompts by combining a system prompt with a task-specific user prompt template. For model inference, a maximum generation length of up to 16,384 tokens is allowed. The tokenizer’s built-in chat template is applied to each prompt to ensure consistent formatting. For each model output we extract the final predicted action sequence enclosed in `<FINAL>` tags.

System Prompt for Evaluation

You are a robot assistant. Your task is to generate a plan given the initial and goal state. A plan is a sequence of actions.

User Prompt for Evaluation

General request###

Your task is to predict a set of actions that arrive at the goal state starting from the initial state. A state is defined by a set of predicates. Predicates can be static (i.e. describe invariant properties of the environment that do not change over time) or dynamic.

Possible Predicates ###: {Your Predicates}

Possible Actions ###: {Your Actions}

Problem to Solve ###: {Initial State} {Goal State}

Output ###: Always output the final plan inside `<FINAL> ... </FINAL>`

Code for Extracting Final Action Sequence

```
def extract_answer(output):
    # This pattern ensures no nested <FINAL> inside the capture
    matches = re.findall(r'<FINAL>((?:(?:?!<FINAL>).)*?)</FINAL>', output, re.DOTALL)
    if matches:
        return re.sub(r'([^\n\s]+)', r'\1', matches[-1]) # last match only
    return None
```

A.2.4 Evaluation Metric Details

We evaluated our models in principle on two metrics: **Success Rate** and **Progress Score**. The formal definitions of the metrics follow:

Given a planning problem,

$$\mathcal{Q} = \langle \mathcal{O}, \mathcal{D}, \mathcal{X}^{(\text{init})}, \mathcal{X}^{(\text{goal})} \rangle,$$

and the model’s prediction,

$$\tau = \{a^{(0)}, \dots, a^{(T-1)}\},$$

we define,

$$\mathcal{X}_N^{(\text{plan})} = \mathcal{X}^{(\text{init})} \times a^{(0)} \times \dots \times a^{(N-1)}.$$

Furthermore, we define that for any action $a^{(i)} \notin$ action space of \mathcal{X} (which is an invalid action),

$$\mathcal{X} \times a^{(i)} = \emptyset,$$

and for all j ,

$$\emptyset \times a^{(j)} = \emptyset.$$

Thus, if the model's predicted plan is valid until m^{th} step, it follows that,

$$m = \min(\{i \mid \mathcal{X}^{(\text{init})} \times a^{(0)} \times \cdots \times a^{(i)} = \emptyset\} \cup \{T\}).$$

We define the logical divergence function to describe similarity between 2 states,

$$f_{\text{logical divergence}}(\mathcal{X}^{(i)}, \mathcal{X}^{(j)}) = \frac{|\mathcal{X}^{(i)} \cap \mathcal{X}^{(j)}|}{|\mathcal{X}^{(i)} \cup \mathcal{X}^{(j)}|}.$$

Finally,

$$\mathbf{Success Rate}(\mathcal{Q}, \tau) = \mathbf{1}[\mathcal{X}_T^{(\text{plan})} \subseteq \mathcal{X}^{(\text{Goal})}] \quad (11)$$

$$\mathbf{Progress Score}(\mathcal{Q}, \tau) = f_{\text{logical divergence}}(\mathcal{X}_m^{(\text{plan})}, \mathcal{X}^{(\text{goal})}) \quad (12)$$

A.3 Training Details

A.3.1 Training Data Details

The training problems are randomly sampled from the generated PDDL domain, with solution lengths ranging from 0 to 60 steps, resulting in a total of 5,807 examples. Among these, 719 are from *Blocks World Align*, 3,048 from *Blocks World Hard*, and 2,038 from *Blocks World Reorder*. For *Blocks World Hard*, the optimal plan lengths follow a 6:2:1:1 ratio across the intervals 0–10, 10–20, 20–30, and 30+ steps. The symbolic solver is permitted to generate both optimal and suboptimal solutions, allowing the model to learn from shortest-path plans as well as alternative, longer trajectories. During training, an evaluation set is held out, consisting of 80, 340, and 227 examples for the respective task types, corresponding to an evaluation ratio of 0.1.

Each training example, consisting of a problem definition and its corresponding solution (either optimal or suboptimal), is provided to the LLM, which then generates a symbolic-language chain-of-thought alignment. These alignments, together with the problems and solutions, form the ground truth of the training dataset. The system prompt used during training is identical to that used in evaluation. Additionally, we allow dynamic rephrasing of the problem setting in the user prompt during training (relative to evaluation) to help the model maintain focus on the problem context. The details of training problem distribution are shown in Figure 5.

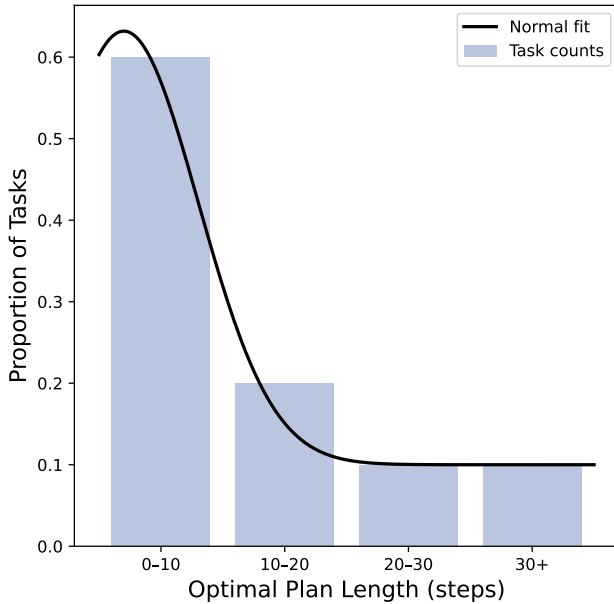


Figure 5: Evaluation data distribution for Blocks World Classic

A.3.2 Training Implementation Details

The pipeline for generating CoT follows a structure similar to the evaluation pipeline, with minor modifications to the prompts and a maximum generation length of 65,536 tokens. From each model output, we extract the final predicted action sequence enclosed within `<REASON>` tags. During the supervised fine-tuning (SFT) stage, the base language model is trained to generate valid action sequences conditioned on planning problem descriptions. We train the model for 5 epochs using a learning rate of 1×10^{-5} with a per-device batch size of 2, applying gradient accumulation over 2 steps to stabilize optimization under limited batch sizes, and optimize all parameters using Adam. For the reinforcement learning stage, we further optimize the SFT model using Constrained Policy Optimization (CPO) with a learning rate of 1×10^{-6} , a KL penalty coefficient $\beta = 0.1$, constraint threshold $d = 0.25$, and constraint weight $\lambda = 0.5$. Training is conducted for 3 epochs with an effective batch size of 4 (via gradient accumulation), using the AdamW optimizer with gradient clipping at 1.0. During online trajectory sampling, the model generates action sequences with temperature 0.6, top- p 0.95, and a maximum of 16,384 new tokens. Logical feasibility violations where action preconditions are not satisfied by the current state are treated as constraints. Each goal

predicate satisfied in the generated state contributes a unit reward, and the total reward is normalized by the number of goal predicates.

System Prompt for Generating Symbolic-language alignment CoT

Role

You are an expert in AI Planning (PDDL) and robotics task modeling. Your task is to generate a detailed chain-of-thought reasoning process for solving the given planning problem.

Goal

You will be provided with:

- The planning domain
- The initial state
- The goal state
- The ground truth task plan

Task Description

Your job is to produce a step-by-step reasoning process that explains:

- Why each action was chosen
- How each action changes the state
- How the evolving state satisfies preconditions and leads toward the goal
- The logical connections between actions, state transitions, and goal achievement
- Explore a few applicable actions at each step other than the provided ground truth
- **After each step, briefly reflect on why alternative actions were not chosen at that point**

Output

You can follow the EXAMPLE reasoning provided, return the full result.

User Prompt for Generating Symbolic-language alignment CoT

Problem Setting: ### {Your Problem Setting}

Task Description Your task is to explain how to predict a set of actions that arrive at the goal state starting the initial state.

Task to explain:

Initial State: {Your Initial State}

Goal State: {Your Goal State}

Correct plan of actions: {Your Symbolic Plan}

Solution: ### After your reasoning, put your final explanation in this format:
{<REASON><ANSWER_HERE></REASON> }

Code for Extracting CoT Response

```
def extract_answer(output):  
    # This pattern ensures no nested <FINAL> inside the capture  
    matches = re.findall(r'<REASON>((?:(!<REASON>).)*?)</REASON>', output, re.DOTALL)  
    if matches:  
        return matches[-1] # last match only  
    return None
```

A.4 More Experiment Results and Analysis

Here we provide the detailed success rate, progress score, and average tokens used of each evaluated model under every task type, including some not listed in main body. By analyzing these results, we conclude a few remarks that are not directly related to our approach but meaningful to share.

Improving Planning Capacities with Recent Models One clear trend is that more recent LLMs exhibit a substantially improved ability to understand symbolic structures and demonstrate clear advantages in planning tasks. Earlier models, such as Qwen-2.5 and Llama-3, show limited understanding of symbolic representations and fail on most planning tasks, despite their larger model scales. In contrast, more recent releases, including Qwen-3, and Mistral, achieve markedly better planning performance. This improvement is likely attributable to the increasing presence of symbolic data in training corpora, as well as the enhanced reasoning capabilities of newer model architectures.

Symbolic Planning Structure as CoT: Symbolic plans provide an effective structural prior for CoT generation. Enforcing symbolic state–transition structure through prompting already reduces token cost and improves planning success, with stronger gains when the model is trained to imitate this structure. SCT-4B achieves both lower token cost and higher success rate. In contrast, CoT distilled from large reasoning models (e.g., 30B-Distill) improves success at the expense of significantly higher token cost. These results show that symbolic-CoT offers a more efficient supervision signal without human curation.

Complementary Roles of SFT and CPO in Learning Planning Behavior Integrating SFT with CPO reveals a clear complementary relationship in learning planning behavior. SFT provides a strong structural prior by imitating valid symbolic reasoning patterns, enabling coherent high-level planning, but imitation alone is insufficient to ensure step-wise feasibility over long horizons. Reinforcement learning, particularly via CPO, complements SFT by explicitly enforcing symbolic state-transition constraints, primarily correcting intermediate transition errors. The larger improvement in progress score reflects reduced accumulation of invalid states that often cause late-stage failures. As a result, the combined SFT+CPO training yields plans that are both more successful and more consistently aligned with symbolic legality.

Table 5: Planning success rate across tasks for all models. Superscripts show improvement, decline, or no change relative to SCT-4B.

Model	Seen Tasks Success Rate			Unseen Tasks Success Rate			Overall Success Rate
	BW Classic	BW Hard	BW Align	Prepare Experiment	Reorganize Room	Machine Parts Assembly	
SCT-4B (ours)	0.60	0.45	0.75	0.45	0.18	0.50	0.46
30B-Distill	0.50 ^{-0.1}	0.31 ^{-0.14}	0.74 ^{-0.01}	0.23 ^{-0.22}	0.16 ^{-0.02}	0.49 ^{-0.01}	0.36 ^{-0.1}
Majority Vote	0.46 ^{-0.14}	0.26 ^{-0.19}	0.49 ^{-0.26}	0.30 ^{-0.15}	0.15 ^{-0.03}	0.39 ^{-0.11}	0.32 ^{-0.14}
Self-Distill	0.45 ^{-0.15}	0.23 ^{-0.22}	0.44 ^{-0.31}	0.25 ^{-0.2}	0.13 ^{-0.05}	0.35 ^{-0.15}	0.28 ^{-0.18}
Prompt-CoT	0.43 ^{-0.17}	0.22 ^{-0.23}	0.45 ^{-0.3}	0.24 ^{-0.21}	0.12 ^{-0.06}	0.33 ^{-0.17}	0.27 ^{-0.19}
SCT _{SFT} -4B	0.58 ^{-0.02}	0.41 ^{-0.04}	0.67 ^{-0.08}	0.42 ^{-0.03}	0.17 ^{-0.01}	0.49 ^{-0.01}	0.43 ^{-0.03}
SCT _{CPO} -4B	0.52 ^{-0.08}	0.33 ^{-0.12}	0.52 ^{-0.23}	0.29 ^{-0.16}	0.17 ^{-0.01}	0.35 ^{-0.15}	0.31 ^{-0.15}
SCT _{DPO} -4B	0.47 ^{-0.13}	0.27 ^{-0.18}	0.49 ^{-0.26}	0.27 ^{-0.18}	0.16 ^{-0.02}	0.36 ^{-0.14}	0.29 ^{-0.17}
SCT _{Symbol} -4B	0.54 ^{-0.06}	0.34 ^{-0.11}	0.84 ^{+0.09}	0.16 ^{-0.29}	0.14 ^{-0.04}	0.50 ^{+0.00}	0.38 ^{-0.08}
Qwen3-30B	0.96 ^{+0.36}	0.70 ^{+0.25}	0.82 ^{+0.07}	0.84 ^{+0.39}	0.47 ^{+0.29}	0.82 ^{+0.32}	0.72 ^{+0.26}
Qwen3-8B	0.48 ^{-0.12}	0.28 ^{-0.17}	0.69 ^{-0.06}	0.33 ^{-0.12}	0.19 ^{+0.01}	0.40 ^{-0.1}	0.35 ^{-0.11}
Qwen3-4B	0.41 ^{-0.19}	0.24 ^{-0.21}	0.42 ^{-0.33}	0.24 ^{-0.21}	0.12 ^{-0.06}	0.34 ^{-0.16}	0.26 ^{-0.2}
Qwen3-1.7B	0.07 ^{-0.53}	0.04 ^{-0.41}	0.01 ^{-0.74}	0.00 ^{-0.45}	0.00 ^{-0.18}	0.00 ^{-0.5}	0.02 ^{-0.44}
Qwen2.5-7B	0.02 ^{-0.58}	0.01 ^{-0.44}	0.01 ^{-0.74}	0.00 ^{-0.45}	0.00 ^{-0.18}	0.00 ^{-0.5}	0.00 ^{-0.46}
Mistral-24B	0.21 ^{-0.39}	0.11 ^{-0.34}	0.71 ^{-0.04}	0.18 ^{-0.27}	0.10 ^{-0.08}	0.12 ^{-0.38}	0.21 ^{-0.25}
Minstral-8B	0.03 ^{-0.57}	0.02 ^{-0.43}	0.05 ^{-0.7}	0.01 ^{-0.44}	0.02 ^{-0.16}	0.02 ^{-0.48}	0.02 ^{-0.44}
Gemma-3-12b	0.09 ^{-0.51}	0.08 ^{-0.37}	0.14 ^{-0.61}	0.06 ^{-0.39}	0.04 ^{-0.14}	0.11 ^{-0.39}	0.08 ^{-0.38}
Gemma-3-4b	0.01 ^{-0.59}	0.01 ^{-0.44}	0.01 ^{-0.74}	0.01 ^{-0.44}	0.01 ^{-0.17}	0.01 ^{-0.49}	0.01 ^{-0.45}
GPT-4o	0.31 ^{-0.29}	0.17 ^{-0.28}	0.54 ^{-0.21}	0.10 ^{-0.35}	0.05 ^{-0.13}	0.11 ^{-0.39}	0.19 ^{-0.27}
SCT-Llama-8B	0.43 ^{-0.17}	0.35 ^{-0.1}	0.64 ^{-0.11}	0.03 ^{-0.42}	0.05 ^{-0.13}	0.13 ^{-0.37}	0.28 ^{-0.18}
Llama-3.1-8B	0.01 ^{-0.59}	0.00 ^{-0.45}	0.01 ^{-0.74}	0.00 ^{-0.45}	0.00 ^{-0.18}	0.00 ^{-0.5}	0.00 ^{-0.46}

Table 6: Planning progress score across tasks for all models. Superscripts show improvement, decline, or no change relative to SCT-4B.

Model	Seen Tasks Progress Score			Unseen Tasks Progress Score			Overall Progress Score
	BW Classic	BW Hard	BW Align	Prepare Experiment	Reorganize Room	Machine Parts Assembly	
SCT-4B (ours)	0.94	0.76	0.95	0.70	0.65	0.84	0.76
30B-Distill	0.71 ^{-0.23}	0.46 ^{-0.3}	0.92 ^{-0.03}	0.41 ^{-0.29}	0.40 ^{-0.25}	0.68 ^{-0.16}	0.54 ^{-0.22}
Majority Vote	0.75 ^{-0.19}	0.59 ^{-0.17}	0.81 ^{-0.14}	0.62 ^{-0.08}	0.55 ^{-0.1}	0.64 ^{-0.2}	0.66 ^{-0.1}
Self-Distill	0.71 ^{-0.23}	0.55 ^{-0.21}	0.75 ^{-0.2}	0.57 ^{-0.13}	0.52 ^{-0.13}	0.62 ^{-0.22}	0.62 ^{-0.14}
Prompt-CoT	0.72 ^{-0.22}	0.57 ^{-0.19}	0.78 ^{-0.17}	0.59 ^{-0.11}	0.54 ^{-0.11}	0.64 ^{-0.2}	0.64 ^{-0.12}
SCT _{SFT} -4B	0.80 ^{-0.14}	0.63 ^{-0.13}	0.91 ^{-0.04}	0.66 ^{-0.04}	0.51 ^{-0.14}	0.74 ^{-0.1}	0.67 ^{-0.09}
SCT _{CPO} -4B	0.85 ^{-0.09}	0.66 ^{-0.1}	0.88 ^{-0.07}	0.61 ^{-0.09}	0.59 ^{-0.06}	0.74 ^{-0.1}	0.69 ^{-0.07}
SCT _{DPO} -4B	0.82 ^{-0.12}	0.63 ^{-0.13}	0.86 ^{-0.09}	0.59 ^{-0.11}	0.58 ^{-0.07}	0.72 ^{-0.12}	0.67 ^{-0.09}
SCT _{Symbol} -4B	0.79 ^{-0.15}	0.58 ^{-0.18}	0.98 ^{+0.03}	0.44 ^{-0.26}	0.46 ^{-0.19}	0.71 ^{-0.13}	0.62 ^{-0.14}
Qwen3-30B	0.95 ^{+0.01}	0.72 ^{-0.04}	0.88 ^{-0.07}	0.89 ^{+0.19}	0.56 ^{-0.09}	0.84 ^{+0.00}	0.76 ^{+0.00}
Qwen3-8B	0.78 ^{-0.16}	0.62 ^{-0.14}	0.93 ^{-0.02}	0.64 ^{-0.06}	0.57 ^{-0.08}	0.72 ^{-0.12}	0.68 ^{-0.08}
Qwen3-4B	0.73 ^{-0.21}	0.58 ^{-0.18}	0.72 ^{-0.23}	0.52 ^{-0.18}	0.52 ^{-0.13}	0.63 ^{-0.21}	0.59 ^{-0.17}
Qwen3-1.7B	0.58 ^{-0.36}	0.46 ^{-0.3}	0.70 ^{-0.25}	0.37 ^{-0.33}	0.46 ^{-0.19}	0.40 ^{-0.44}	0.47 ^{-0.29}
Qwen2.5-7B	0.51 ^{-0.43}	0.46 ^{-0.3}	0.75 ^{-0.2}	0.43 ^{-0.27}	0.49 ^{-0.16}	0.45 ^{-0.39}	0.50 ^{-0.26}
Mistral-24B	0.51 ^{-0.43}	0.37 ^{-0.39}	0.95 ^{+0.00}	0.35 ^{-0.35}	0.35 ^{-0.3}	0.58 ^{-0.26}	0.49 ^{-0.27}
Minstral-8B	0.22 ^{-0.72}	0.14 ^{-0.62}	0.19 ^{-0.76}	0.07 ^{-0.63}	0.18 ^{-0.47}	0.17 ^{-0.67}	0.14 ^{-0.62}
Gemma-3-12b	0.64 ^{-0.3}	0.53 ^{-0.23}	0.83 ^{-0.12}	0.49 ^{-0.21}	0.50 ^{-0.15}	0.53 ^{-0.31}	0.56 ^{-0.2}
Gemma-3-4b	0.51 ^{-0.43}	0.43 ^{-0.33}	0.69 ^{-0.26}	0.34 ^{-0.36}	0.41 ^{-0.24}	0.35 ^{-0.49}	0.44 ^{-0.32}
GPT-4o	0.68 ^{-0.26}	0.54 ^{-0.22}	0.88 ^{-0.07}	0.41 ^{-0.29}	0.45 ^{-0.2}	0.49 ^{-0.35}	0.55 ^{-0.21}
SCT-Llama-8B	0.84 ^{-0.1}	0.79 ^{+0.03}	0.93 ^{-0.02}	0.46 ^{-0.24}	0.51 ^{-0.14}	0.78 ^{-0.06}	0.72 ^{-0.04}
Llama-3.1-8B	0.54 ^{-0.4}	0.46 ^{-0.3}	0.80 ^{-0.15}	0.45 ^{-0.25}	0.48 ^{-0.17}	0.46 ^{-0.38}	0.51 ^{-0.25}

Table 7: Planning token count across tasks for all models. Superscripts show **improvement**, **decline**, or no change relative to SCT-4B.

Model	Seen Tasks Token Count			Unseen Tasks Token Count			Overall
	BW Classic	BW Hard	BW Align	Prepare Experiment	Reorganize Room	Machine Parts Assembly	
SCT-4B (ours)	5521	8437	5298	7654	8312	6341	7543
30B-Distill	9101 ^{+3,580}	10785 ^{+2,348}	5558 ⁺²⁶⁰	10624 ^{+2,970}	10788 ^{+2,476}	7560 ^{+1,219}	9555 ^{+2,012}
Majority Vote	21856 ^{+16,335}	34192 ^{+25,755}	20834 ^{+15,536}	31024 ^{+23,370}	32576 ^{+24,264}	25712 ^{+19,371}	29864 ^{+22,321}
Self-Distill	5895 ⁺³⁷⁴	8723 ⁺²⁸⁶	5412 ⁺¹¹⁴	7891 ⁺²³⁷	8567 ⁺²⁵⁵	6589 ⁺²⁴⁸	7698 ⁺¹⁵⁵
Prompt-CoT	7234 ^{+1,713}	9845 ^{+1,408}	6123 ⁺⁸²⁵	9034 ^{+1,380}	9512 ^{+1,200}	7856 ^{+1,515}	8694 ^{+1,151}
SCTsFT-4B	5536 ⁺¹⁵	8448 ⁺¹¹	5391 ⁺⁹³	7686 ⁺³²	8348 ⁺³⁶	6316 ⁻²⁵	7584 ⁺⁴¹
SCTcpo-4B	5042 ⁻⁴⁷⁹	6345 ^{-2,092}	4650 ⁻⁶⁴⁸	5887 ^{-1,767}	6795 ^{-1,517}	5610 ⁻⁷³¹	6012 ^{-1,531}
SCTDPO-4B	5610 ⁺⁸⁹	8572 ⁺¹³⁵	5413 ⁺¹¹⁵	7792 ⁺¹³⁸	8390 ⁺⁷⁸	6203 ⁻¹³⁸	7621 ⁺⁷⁸
SCTSymbol-4B	7689 ^{+2,168}	10328 ^{+1,891}	4483 ⁻⁸¹⁵	10876 ^{+3,222}	9908 ^{+1,596}	7494 ^{+1,153}	9107 ^{+1,564}
Qwen3-30B	9435 ^{+3,914}	11418 ^{+2,981}	9612 ^{+4,314}	9948 ^{+2,294}	11923 ^{+3,611}	10339 ^{+3,998}	10868 ^{+3,325}
Qwen3-8B	8564 ^{+3,043}	9368 ⁺⁹³¹	6409 ^{+1,111}	8413 ⁺⁷⁵⁹	8983 ⁺⁶⁷¹	8510 ^{+2,169}	8631 ^{+1,088}
Qwen3-4B	8409 ^{+2,888}	9963 ^{+1,526}	6657 ^{+1,359}	8319 ⁺⁶⁶⁵	9323 ^{+1,011}	8316 ^{+1,975}	8929 ^{+1,386}
Qwen3-1.7B	7133 ^{+1,612}	7440 ⁻⁹⁹⁷	6518 ^{+1,220}	7268 ⁻³⁸⁶	6980 ^{-1,332}	5917 ⁻⁴²⁴	7000 ⁻⁵⁴³
Qwen2.5-7B	563 ^{-4,958}	905 ^{-7,532}	560 ^{-4,738}	1165 ^{-6,489}	570 ^{-7,742}	550 ^{-5,791}	794 ^{-6,749}
Mistral-24B	894 ^{-4,627}	1089 ^{-7,348}	853 ^{-4,445}	906 ^{-6,748}	785 ^{-7,527}	717 ^{-5,624}	920 ^{-6,623}
Minstral-8B	2871 ^{-2,650}	3195 ^{-5,242}	1952 ^{-3,346}	2707 ^{-4,947}	1847 ^{-6,465}	2001 ^{-4,340}	2547 ^{-4,996}
Gemma-3-12b	582 ^{-4,939}	704 ^{-7,733}	563 ^{-4,735}	732 ^{-6,922}	550 ^{-7,762}	617 ^{-5,724}	653 ^{-6,890}
Gemma-3-4b	765 ^{-4,756}	926 ^{-7,511}	772 ^{-4,526}	953 ^{-6,701}	772 ^{-7,540}	909 ^{-5,432}	883 ^{-6,660}
GPT-4o	2590 ^{-2,931}	2761 ^{-5,676}	2790 ^{-2,508}	2791 ^{-4,863}	2640 ^{-5,672}	2796 ^{-3,545}	2757 ^{-4,786}
SCT-Llama-8B	5912 ⁺³⁹¹	8234 ⁻²⁰³	5567 ⁺²⁶⁹	7823 ⁺¹⁶⁹	8156 ⁻¹⁵⁶	6512 ⁺¹⁷¹	7534 ⁻⁹
Llama-3.1-8B	8234 ^{+2,713}	9156 ⁺⁷¹⁹	6387 ^{+1,089}	8412 ⁺⁷⁵⁸	8876 ⁺⁵⁶⁴	8234 ^{+1,893}	8523 ⁺⁹⁸⁰

A.5 Overall pipeline pseudo code

Algorithm 1 Full Planning Pipeline

```

1: procedure FULLPLANPIPELINE( $O, M_0, \Psi, U, N$ )
2:    $(\hat{P}, \hat{A}) \leftarrow \Psi_{M_0}(U)$  ▷ Generate predicates/actions
3:    $\hat{D} \leftarrow (\hat{P}, \hat{A})$  ▷ Construct domain
4:    $\mathcal{C} \leftarrow \emptyset$  ▷ Problem–CoT pairs
5:   for  $i = 1$  to  $N$  do
6:      $(X^{init}, X^{goal}) \leftarrow \text{RANDOMSAMPLE}(O, \hat{D})$ 
7:      $Q_i \leftarrow (O, \hat{D}, X^{init}, X^{goal})$ 
8:      $\tau \leftarrow \text{PDDL\_SOLVER}(Q_i)$ 
9:      $\text{CoT}_\tau \leftarrow \{f_{M_0}^{NL}(X^t, a^t, X^{t+1})\}_{t=0}^{T-1}$ 
10:     $\mathcal{C} \leftarrow \mathcal{C} \cup \{(Q_i, \text{CoT}_\tau)\}$ 
11:   end for
12:    $M_{SFT} \leftarrow \text{SFT}(M_0, \mathcal{C})$  ▷ Supervised fine-tuning on CoT corpus
13:    $M_{SCT} \leftarrow \text{RL}(M_{SFT}, \hat{D})$  ▷ RL with domain  $\hat{D}$  as reward signal
14:   Scores  $\leftarrow \emptyset$ 
15:   for  $Q_j \in \text{TestSet}$  do
16:      $\hat{y} \leftarrow M_{SCT}(Q_j)$ 
17:      $\hat{\tau} \leftarrow \text{EXTRACTPLAN}(\hat{y})$ 
18:     Scores  $\leftarrow \text{Scores} \cup \{\text{PLANVALIDATION}(\hat{\tau}, Q_j)\}$ 
19:   end for
20:    $\text{Score}_{avg} \leftarrow \frac{1}{|\text{Scores}|} \sum \text{Scores}$ 
21:   return  $M_{SCT}, \text{Score}_{avg}$ 
22: end procedure

```

A.6 Example LLM-generated PDDL Domain

System Prompt for Generating CoT

```
(define (domain LLM_generated_domain)
  (:requirements :strips :equality)
  (:predicates
    (obj ?b1)
    (on-table ?b1 ?t1)
    (holding ?b1 ?r1)
    (hand_free ?r1)
    (top ?b2)
    (above ?b1 ?b2)
    (robot ?r1)
    (table ?t1)
    (aligned ?b1 ?b2)
  )

  (:action pick-up
    :parameters (?b1 ?t1 ?r1)
    :precondition (and (obj ?b1) (robot ?r1) (on-table
      ?b1 ?t1) (top ?b1) (hand_free ?r1) (table ?t1))
    :effect (and (not (hand_free ?r1)) (not (on-table
      ?b1 ?t1)) (holding ?b1 ?r1))
  )

  (:action stack
    :parameters (?b1 ?b2 ?r1)
    :precondition (and (obj ?b1) (top ?b1) (holding ?b1
      ?r1) (robot ?r1) (top ?b2) (obj ?b2))
    :effect (and (above ?b1 ?b2) (hand_free ?r1) (not
      (top ?b2)) (not (holding ?b1 ?r1)))
  )

  (:action unstack
    :parameters (?b1 ?b2 ?r1)
    :precondition (and (obj ?b1) (robot ?r1) (top ?b1)
      (above ?b1 ?b2) (hand_free ?r1) (obj ?b2))
    :effect (and (not (hand_free ?r1)) (not (above ?b1
      ?b2)) (top ?b2) (holding ?b1 ?r1))
  )

  (:action put-down
    :parameters (?b1 ?t1 ?r1)
    :precondition (and (obj ?b1) (holding ?b1 ?r1) (top
      ?b1) (robot ?r1) (table ?t1))
    :effect (and (hand_free ?r1) (not (holding ?b1 ?r1))
      (on-table ?b1 ?t1))
  )

  (:action rotate
    :parameters (?b1 ?b2 ?t1 ?r1)
    :precondition (and (table ?t1) (robot ?r1) (obj ?b2)
      (obj ?b1) (on-table ?b2 ?t1) (holding ?b1 ?r1))
    :effect (and (aligned ?b1 ?b2))
  )
)
```

A.7 Real Robot Experiment Implementation Details

The real robot experiment follows a three-stage pipeline: perception, planning, and execution. First, we extract the initial logical state of the scene using either a VLM or a rule-based classifier. Next, SCT-4B generates a subtask plan. Finally, the plan is dispatched to the UR5e controller for execution.

Throughout the experiment, goal states, object positions, and subtask execution routines are predefined and treated as ground truth.

A.7.1 Initial State Perception

VLM We use Qwen3-4B-VL-Instruct(Bai et al., 2025) as the visual perception module. The model receives a single RGB image of the scene together with a predicate vocabulary and directly outputs a set of PDDL predicates representing the initial logical state. The prompt supplies the image and the list of admissible predicates; the model returns the subset that holds in the depicted scene. An example prompt is shown below.

```
VLM Perception Prompt

You are given views of a table-top scene with cups.
Describe the state of every object you see within the PDDL
domain. This will be used as the initial state of a pddl
problem.

## PDDL Domain ##
A state is defined by a set of predicates.
Possible Predicates in Domain: on-table, holding, hand_free,
top, above, beside, nothing_beside
Possible objects: robot, table, drawer, and some objects
Possible Actions in Domain:
- [pick-up, b, t, r]: take b from table t; requires [top,
b], [on-table, b, t], [hand_free, r]
- [put-down, b, t, r]: place b on table t; requires
[holding, b, r]
- [unstack, b1, b2, r]: remove b1 from b2; requires [top,
b1], [above, b1, b2], [hand_free, r]
- [stack, b1, b2, r]: place b1 on b2; requires [holding, b1,
r], [top, b2]
- [align, b1, b2, t, r]: place beside on table t; requires
[holding, b1, r], [on-table, b2, t], [nothing_beside, b2]

Initially, the drawer is open, and robot is hand_free.

The goal state of the problem is: [hand_free, robot],
[above, mouse, drawer], [top, mouse], [above, pink_cup,
drawer], [above, grey_cup, pink_cup], [above, white_cup,
grey_cup], [top, white_cup], [above, green_box, drawer],
[top, green_box], [above, red_box, drawer], [top, red_box]

You need to provide the initial state based on the image of
this problem.
return you final answers in <FINAL>your final
predicates</FINAL>
```

Rule-based classifier. As an upper-bound perception baseline we use ground-truth 6-DoF object poses obtained from the robot workspace. Geometric rules map spatial relationships to PDDL predicates: for example, `on-table(obj, tbl)` is asserted when the object's z -coordinate is within a threshold of the table surface, and `holding(obj, robot)` is asserted when the gripper is closed around the object.

A.7.2 Subtask-plan Generation

The extracted initial state is passed to SCT-4B together with a predefined goal state, using the same evaluation prompt format described in Section A.2.3. The model generates a chain-of-thought reasoning trace followed by a final action sequence enclosed in `<FINAL>` tags.

A.7.3 Low-level Execution

Each PDDL action in the generated plan is mapped to a predefined pick-and-place skill with known object positions. The UR5e arm is controlled via the RTDE library, which sends target joint configurations and Cartesian waypoints to the robot controller.

A.8 VLA Implementation Details

To further investigate the application of high-level planners in robotic tasks, we integrate our SCT-4B model with the π_0 model (Black et al., 2024), which serves as the low-level executor, to control a UR5e robot in a set of table-organization tasks within our real-robot experiment.

The SCT-4B model produces high-level commands expressed in PDDL, which are passed to the π_0 model. The π_0 model, fine-tuned on 200 real-world pick-and-place trajectories using PDDL-based prompts, translates these plans into low-level spatial delta poses for the UR5e. Execution is then handled by the UR5e’s built-in controllers.

The overall task involves picking up and placing objects in different locations to place everything in place and reach a required table-top configuration. This VLA experiment serves as a proof of concept, demonstrating that our high-level planners can be seamlessly connected to a lower-level VLA model to carry out real-world tasks.

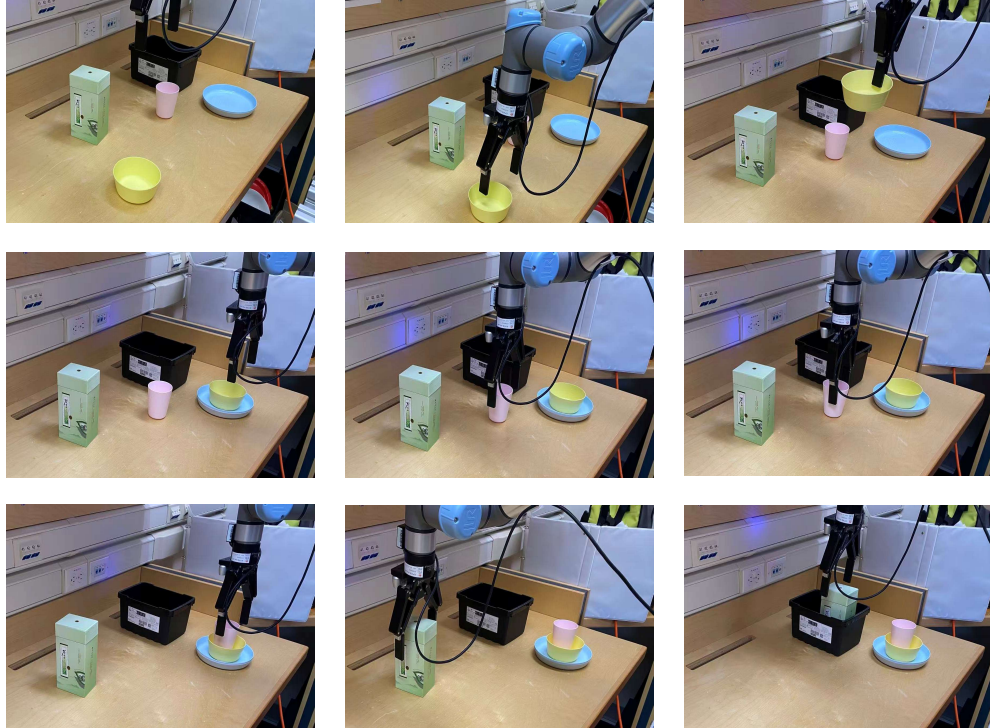


Figure 6: SCT-4B performing room organization task together with π_0

A.9 Backbone Ablation

To assess the generality of SELF-CRITeach (SCT) beyond the Qwen family, we applied the full pipeline to Llama-3.1-8B, which differs substantially from Qwen in both architecture and training recipe. Integrating SCT yields substantial improvements in both success rate and progress score, indicating gains not only in task completion but also in planning quality for partially solved tasks. While the improvements on unseen tasks are smaller, SCT still provides consistent benefits. These cross-model results show that SCT is not tied to Qwen and can effectively strengthen a broad range of LLMs, including those that start with weaker symbolic-planning capabilities.

Table 8: Model planning success rate comparing before/after fine-tuning on Llama model. Superscripts show **improvement**, **decline**, or no change relative to Llama-3.1-8B.

Model	Seen Tasks Success Rate			Unseen Tasks Success Rate			Overall Success Rate
	BW Classic	BW Hard	Align	Prepare Experiment	Reorganize Room	Machine Parts Assembly	
SCT-Llama-8B (ours, base)	0.427	0.351	0.642	0.032	0.048	0.132	0.277
Llama-3.1-8B	0.005 ^{-0.42}	0.003 ^{-0.35}	0.013 ^{-0.63}	0.000 ^{-0.03}	0.000 ^{-0.05}	0.000 ^{-0.13}	0.003 ^{-0.27}

Table 9: Model progress score comparing before/after fine-tuning on Llama model. Superscripts show **improvement**, **decline**, or no change relative to Llama-3.1-8B.

Model	Seen Tasks Progress Score			Unseen Tasks Progress Score			Overall Progress Score
	BW Classic	BW Hard	Align	Prepare Experiment	Reorganize Room	Machine Parts Assembly	
SCT-Llama-8B (ours, base)	0.837	0.785	0.932	0.463	0.512	0.775	0.716
Llama-3.1-8B	0.538 ^{-0.3}	0.463 ^{-0.32}	0.800 ^{-0.13}	0.447 ^{-0.02}	0.484 ^{-0.03}	0.462 ^{-0.31}	0.512 ^{-0.2}